K/ER-306

Energy Systems Environmental Restoration Program

# Microgravity Survey of the Oak Ridge K-25 Site, Oak Ridge, Tennessee

R. D. Kaufmann



Date Issued—May 1996



Prepared for the
U.S. Department of Energy
Office of Environmental Management
under budget and reporting codes EU 20 and EW 20

DISTRIBUTION OF THIS DOCUMENT IS UNLIMITED

Environmental Management Activities at the
OAK RIDGE K-25 SITE
Oak Ridge, Tennessee 37831
managed by
LOCKHEED MARTIN ENERGY SYSTEMS, INC.
for the
U.S. DEPARTMENT OF ENERGY
under contract DE-AC05-84OR21400

# PREFACE

*Microgravity Survey of the Oak Ridge K-25 Site, Oak Ridge, Tennessee*, was prepared to document site characterization data collected during scoping phase investigations in accordance with requirements under the Comprehensive Environmental Response, Compensation, and Liability Act. This work was performed under Work Breakdown Structure 1.4.12.4.1.05.03.03, Activity Data Sheet 4305, "K-25 Groundwater Program." Scoping phase data are collected to support ongoing and future remedial investigations on the K-25 Site. The data discussed in this report will be summarized in the Oak Ridge K-25 Site Groundwater Remedial Site Evaluation Report, currently in preparation.

# ACKNOWLEDGMENTS

This research for this document, *Microgravity Survey of the Oak Ridge K-25 Site, Oak Ridge, Tennessee*, was supported in part by an appointment to the U.S. Department of Energy Laboratory Cooperative Postgraduate Research Training Program at the Oak Ridge National Laboratory administered by the Oak Ridge Institute for Science and Education. Bill Doll, Peter Lemiszki, and Tom Zondlo provided valuable assistance in modeling the gravity data and improved the writing of this report through their insightful reviews of the manuscript. The author would like to thank Jeff Wilson, who provided the terrain correction code developed by Environmental Consulting Engineers, Inc., and Brian Murray (Science Applications International Corporation), who provided borehole data from the K-901 area.

# CONTENTS

# FIGURES

## TABLES

# EXECUTIVE SUMMARY

Karst features are known to exist within the carbonate bedrock of the Oak Ridge K-25 Site and may play an important role in groundwater flow and contaminant migration. Microgravity is an optimal geophysical tool for the detection and delineation of subsurface cavities within the karstified rocks. In this study, a microgravity survey of the K-25 Site reveals gravity anomalies that are modeled as bedrock density contrasts, regolith thickness variations, and mud-filled cavities.

The data were acquired along profile lines and at areally distributed points throughout the site. The gravity anomalies along individual profile lines are modeled using density and regolith thickness constraints provided by boreholes. The gravity data are contoured to produce a Bouguer gravity map of the K-25 Site, which shows a correlation with the mapped geology and provides new insights on the lithology and structure location.

Large gravity lows within the Kingsport Formation and Mascot Dolomite are modeled as areas of intense karstification and may represent portions of a major groundwater conduit. A gravity anomaly located within a syncline correlates with a mapped area of thick regolith cover. An area of low gravity located north of the syncline axis is modeled as a change in Chickamauga bedrock density related to greater karstification. Gravity data within the mapped Rome thrust slice bounded by the K-25 fault suggests that a northeast dipping Conasauga lithology may exist within the northern section of the slice, and that the karstified Chickamauga bedrock north of the syncline axis may continue east beneath the slice. Data from this study combined with data from previous surveys of the K-901 area, located in the northwest corner of the K-25 Site, reveal a southwest trending gravity low associated with a highly karstified Knox bedrock within the K-901 area.

The gravity anomalies modeled as subsurface cavities show the locations where karst may affect groundwater flow and have the potential of causing sinkholes. The gravity models are nonunique and should serve as a guide for future geophysical surveys and drilling to further constrain the subsurface structure. The combination of gravity mapping and seismic reflection profiling (in progress) may help to enhance the current geologic map of K-25.

# 1. INTRODUCTION

This report discusses the results of a microgravity survey of the Oak Ridge K-25 Site. The main objective of the survey is to identify areas containing bedrock cavities. Secondary objectives included correlating the observed gravity to the geology and to variations in overburden thickness. The analysis includes 11 profile lines that are oriented perpendicular to the geologic strike and major structures throughout the K-25 Site. The profile lines are modeled in an effort to relate gravity anomalies to karst features such as concentrations of mud-filled cavities. Regolith thickness and density data provided by boreholes constrain the models. Areally distributed points are added to the profile lines to produce a gravity contour map of the site. In addition, data from the K-901 area are combined with data from previous surveys to produce a high resolution map of that site.

The K-25 Site is located in an area of folded and faulted sedimentary rocks within the Appalachian Valley and Ridge physiographic province. Paleozoic age rocks of the Rome Formation, Knox Group, and Chickamauga Supergroup underlie the K-25 Site and contain structures that include the Whiteoak Mountain Fault, the K-25 Fault, a syncline, and an anticline. The mapped locations of the rock units and complex structures are currently derived from outcrop and well log analysis, and are shown in Fig.1-1.

The geologic mapping and bedrock well logging identified a number of karst features within the carbonate rocks (Lemiszki 1994). The location of the karst features, rock units, and structures are important parameters in the hydrogeologic modeling of the K-25 Site. Results from this study, combined with results from geologic investigations and ongoing seismic reflection profiling, will help to better define these parameters and may indicate areas warranting further investigation.

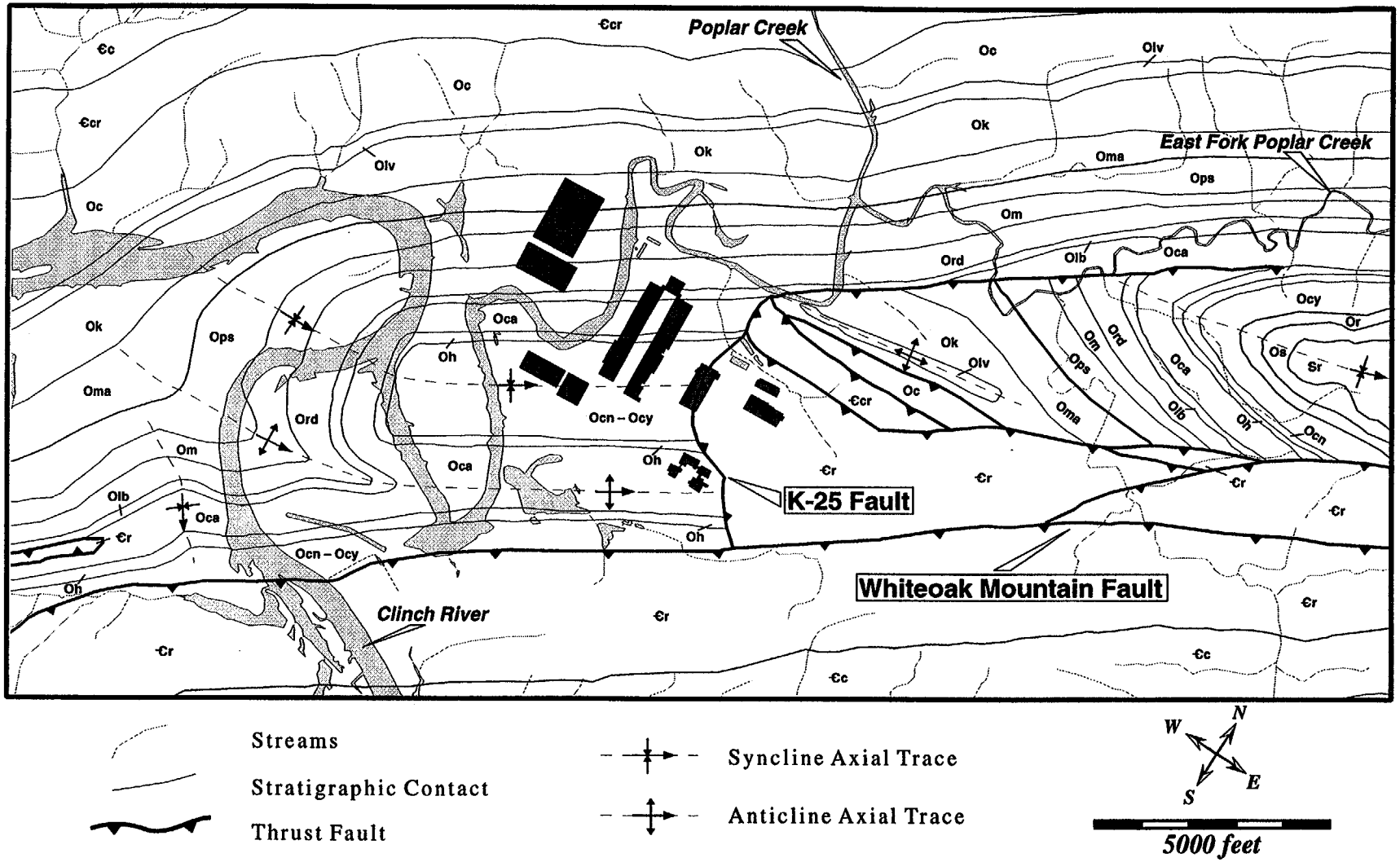


**Fig. 1-1. Bedrock geologic map of the K-25 Site.**

# 2. MICROGRAVITY SURVEY

## 2.1 METHOD

Microgravity surveying is one of the most promising surface geophysical methods for detection and delineation of subsurface cavities (Butler 1991). For example, a microgravity survey conducted at the Y-12 Plant on the Oak Ridge Reservation by Carpenter et al. (1995) was effective in characterizing a bedrock cavity intersected by a monitoring well. The method involves finding anomalies in the local gravitational field of the earth due to lateral variations in the subsurface density structure.

Detectable structures include near-surface cavities, overburden variations, bedrock lithologic contrasts, and deep crustal features. Because the gravitational field of the earth is affected by all subsurface variations in density, there is an inherent ambiguity in determining the source of a gravity anomaly (i.e., a small, shallow cavity can produce the same anomaly as a large, deep cavity). However, by using available information such as overburden thickness and density measurements as constraints, the effects of shallow, small-scale features may be modeled and fit to the observed gravity data.

Microgravity data are acquired using a noninvasive instrument that measures the vertical component of the acceleration of gravity at discrete points on the earth's surface. The relative difference in gravity between a base station and a field station is measured, not the absolute gravity. The standard unit for the acceleration of gravity is the Gal (1 Gal = 0.01 $m/s^2$). The average value of the acceleration of gravity at the earth's surface is approximately 980 Gal. Microgravimeters are capable of measuring with a precision of $10^{-6}$ Gal (1 $\mu$Gal).

Stations in a microgravity survey are usually arranged in a profile line or a grid pattern. The spacing between stations is chosen to adequately sample the expected gravity anomalies. The elevations of the stations must be accurately surveyed to at least 0.1 ft to account for the decrease in gravity with increasing elevation. Base stations must be established and frequently reoccupied to account for the instrument drift. Typically, a field base station is established that is within a convenient distance from the measurement stations. The difference in gravity between the field base station and the main base station is found by taking many readings between the two. In this fashion, all the points in a survey are tied to a single main base station with gravity values relative to it.

After collecting the gravity survey data, corrections are applied to the data that take into account instrument drift, variations in latitude, tidal forces, elevation, and topography (Telford et al. 1976). Frequent reoccupation of a base station will account for instrument drift due to elastic aging of the internal spring, weather conditions, and other effects. A latitude correction is applied to the data to account for the centrifugal acceleration due to the spinning of the earth and the slight equatorial bulge. The effects of tidal forces are removed based upon the time and date of each measurement. A correction for the decrease in gravity with elevation is applied to the data, and all measurements are reduced to a common datum such as sea level. After removing the effects of the mass between the datum and measurement point, the resulting values are known as the *simple Bouguer gravity*. Variations in the topography, such as nearby hills and valleys, will always act to decrease the Bouguer gravity. This effect is determined with the *terrain correction*, and the corrected values are known as *complete Bouguer gravity*.

Deviations from a uniform complete Bouguer gravity value are defined as *Bouguer gravity anomalies* and are directly attributable to lateral changes in the subsurface density. Components of the gravity anomalies, however, may be due to deep, regional features, which are typically not of interest in

a local microgravity study. The regional components have a large spatial wavelength compared with anomalies due to shallower, localized features. To isolate the anomalies due to local features, the regional component must be removed from the data. This is normally accomplished by removing a linear or planar trend from the data and is illustrated in Fig. 2-1.

The amplitude and spatial wavelength of the gravity anomalies are controlled by the size, depth, and density contrast of the subsurface features. To determine the depth and size of the feature, a model must be developed that uses realistic density contrasts and applies available constraints. The gravity anomalies may then be interpreted by matching the data to the forward model.

## 2.2 INSTRUMENTATION

A LaCoste and Romberg (L&R) Model D microgravimeter was used to collect data between February 3, 1995 and September 1, 1995, which covers three separate rental periods of the gravity meter. The rentals consisted of L&R meters D-46 and D-2 from J. D. Fett Instruments. The meter measures the relative difference in the force of gravity between stations by nulling the tension on a spring connected to a mass within the meter. The gravity values may be read to a precision of 1 μGal, and under field conditions are accurate to between ±3 to ±6 μGal (Butler 1991). Further details on the instrument may be found in the L&R instruction manual (L&R 1991).

## 2.3 GRAVITY METER COMPARISON

The K-25 gravity data, acquired with the two different L&R Model D microgravimeters, were combined with data from previous surveys in the K-901 area. The K-901 data were acquired with a L&R Model D microgravimeter (Wilson and Ketelle 1992) and a Scintrex CG-3 microgravimeter (Coleman Energy & Environmental Systems 1994). Theoretically, the values from different meters may be related to each other by simply removing a static shift from the data sets. The static shift is the difference between gravity measurements at the same station acquired with different meters.

In order to compare the relative accuracy and precision of the gravity meters, data were acquired at five stations within a building at ORNL using both a L&R Model D and Scintrex CG-3 microgravimeter. The stations were occupied six times with each meter to obtain the average and standard deviation of the measurements. The following table summarizes the results of the test.

**Table 2-1. Comparison of average gravity values and standard deviations (σ) obtained with the L&R Model D and Scintrex CG-3 microgravimeters**

| Sta | L&R Grav (μGals) | σ (μGals) | Scintrex Grav (μGals) | σ (μGals) |
|---|---|---|---|---|
| BASE | 100 | --- | 100 | --- |
| A | 108 | 4 | 106 | 3 |
| B | 87 | 5 | 79 | 2 |
| C | 79 | 6 | 77 | 6 |
| D | 81 | 3 | 78 | 3 |
| E | 114 | 6 | 108 | 2 |

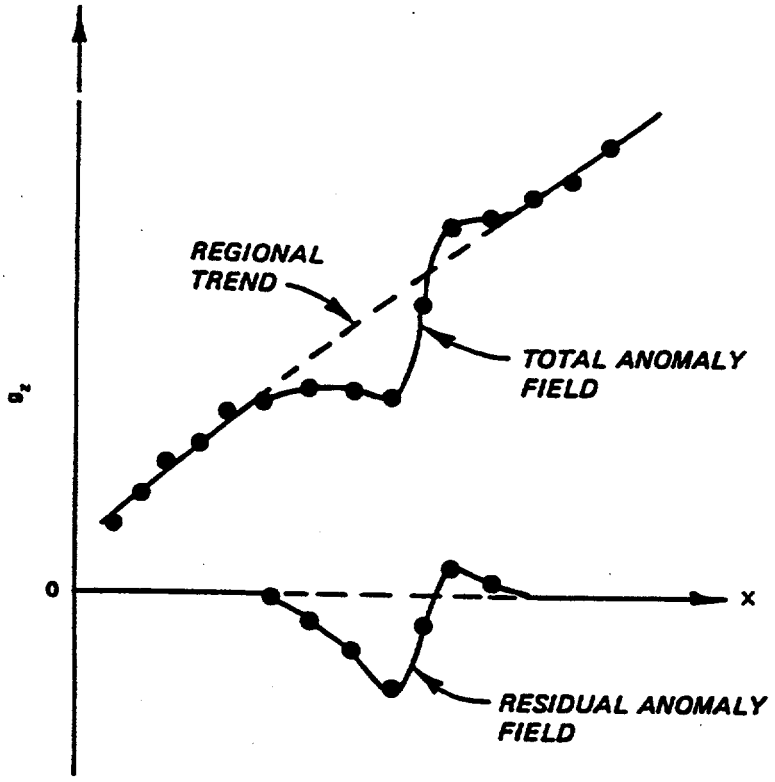


**Fig. 2-1. Illustration of region removal (after Butler 1991).**

The average difference in gravity readings between the two meters is 4 μGals, which is within the average standard deviation of 5 μGals for the L&R Model D meter. The Scintrex CG-3 meter proved to be slightly more repeatable, with an average standard deviation of 3 μGals. The standard deviations would probably be slightly higher under field conditions due to meter leveling errors and vibrationally noisy environments.

The test shows that the L&R Model D and Scintrex CG-3 microgravimeters will show the same relative differences in gravity with approximately the same level of accuracy. It is important to note that the data in the previous survey using the Scintrex CG-3 microgravimeter (Coleman Energy & Environmental Systems 1994) were acquired with a precision of only 10 μGals, while the L&R data were acquired with a precision of 1 μGal. In future microgravity surveys, data from all instruments should be acquired with a precision of 1 μGal to ensure that the highest possible accuracy is attained.

## 2.4 DETECTABILITY

Before any data were collected, the gravitational response of shallow cavities was modeled to ensure that these cavities might be detected and to design optimal survey parameters. Both the magnitude and spatial wavelength of an anomaly were considered in this analysis. Based on the expected accuracy of the L&R meter under field conditions, a detection threshold of 10 μGals was assumed.

Cavities within limestone and dolomite are the main targets of this survey. The density contrast between a cavity and the surrounding rock will vary depending on the material filling the cavity. Fig. 2-2 shows the maximum depth that a spherical cavity within dolomite bedrock can be detected as a function of its radius and density contrast. The depth is reported as the depth to the center of the cavity. The model indicates that an air-filled cavity with a radius of 5 ft is detectable to a depth of 16 ft, but an air-filled cavity with a radius of 10 ft is detectable to a depth of 48 ft. Cavities with smaller density contrasts have shallower maximum detectable depths for a given radius.

The station spacings for the survey must be sufficiently close to define the anomalies resulting from cavities. As a general rule, the station spacing must be no more than one-half the anomaly wavelength. Fig. 2-3 shows the calculated anomalies for spherical, mud-filled cavities of three different sizes. The depth to the center of the cavities is fixed at 20 ft and represents a shallow cavity depth reported in well logs (Geraghty & Miller, Inc. 1989). The model shows that a 5-ft mud-filled cavity is not detectable at this depth. A 10-ft mud-filled cavity at this depth is detectable, but requires closely spaced (~10 ft) stations. A 15-ft mud-filled cavity at this depth produces an 85-μGal anomaly that requires stations spaced approximately 25 ft apart to adequately define the anomaly.

In reality, many cavities of varying density contrast, size, shape, and depth may exist in a localized area and collectively produce a gravity anomaly that has a similar size and wavelength as one produced by a single large cavity. Considering the models described above and the cost of each data point acquisition, it was decided that a station spacing of 25-50 ft would be adequate to define anomalies resulting from large cavities (e.g., mud-filled, spherical cavities with radii >15 ft at 20 ft depth) or areas with concentrations of smaller cavities. Additional stations may be added in future studies to further define large anomalies and to identify anomalies resulting from individual small cavities.

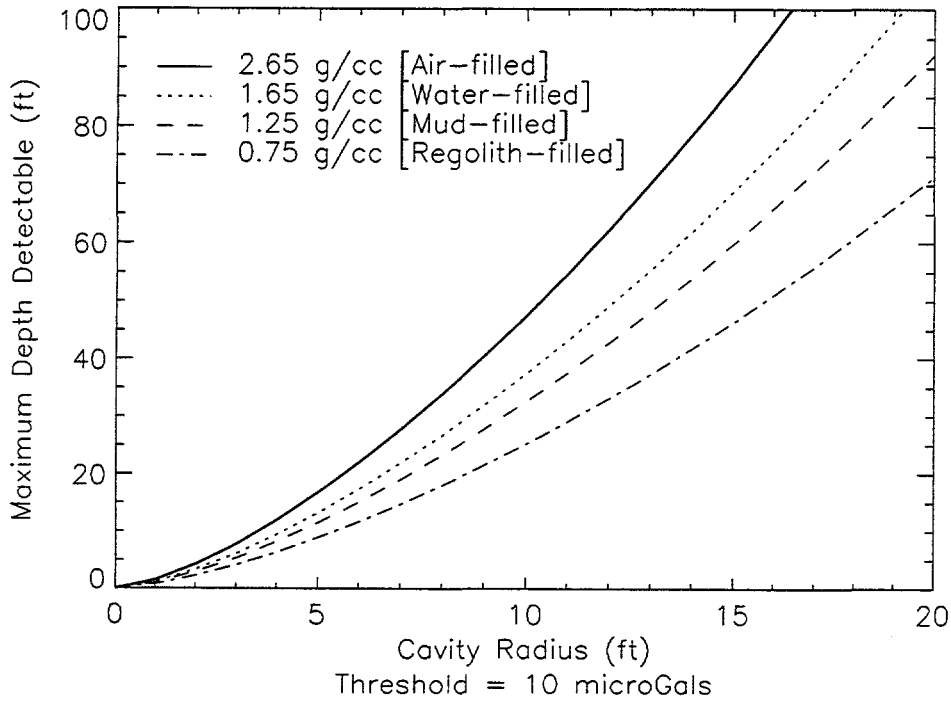


**Fig. 2-2. Maximum depth to the center of a spherical cavity detectable by the microgravimeter as a function of the cavity's radius and density contrast.**

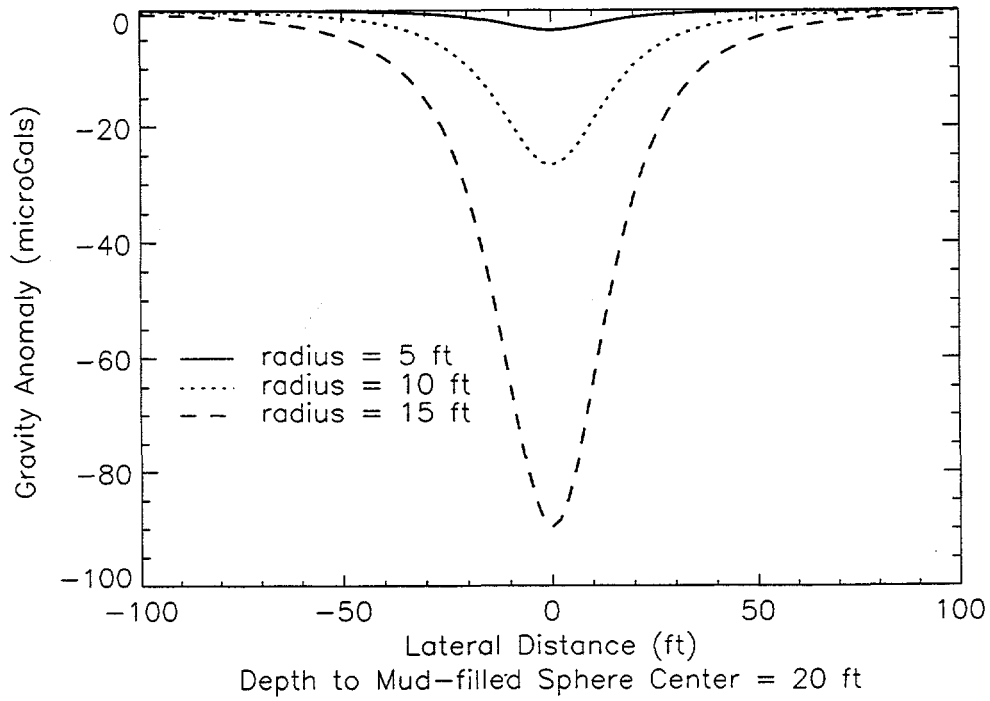


**Fig. 2-3. Calculated gravity anomaly of a mud-filled, spherical cavity with a density contrast of -1.25 g/cc.**

## 2.5 CAVE TESTS

Profile lines were acquired over two air-filled caves on the Oak Ridge Reservation as a detectability test. The two caves, Copper Ridge Cave and Rennie's Cave, both formed in the Copper Ridge Dolomite of the Knox Group. Copper Ridge Cave is located on Copper Ridge, and Rennie's Cave is located on Chestnut Ridge. Figs. 2-4 and 2-5 show the maps of the caves with the location of the gravity survey profiles. The profile lines are perpendicular to the cave passage, and have station spacings of 10-20 ft. Relative elevations were surveyed with an uncertainty of 1-2 mm, which only contributes approximately 0.2-0.4 μGals of error to the observations.

The Copper Ridge Cave profile line strikes east to west, and crosses over the cave approximately 80 ft south of the cave entrance. At this point, the cave ceiling is estimated to be 20 ft below the ground surface. The air-filled cave is modeled to be roughly cylindrical in shape, with a diameter of approximately 10 ft and a density contrast of -2.7 g/cc with the surrounding dolomite. Fig. 2-6 shows the observed gravity anomaly and the calculated anomaly using the estimated position of the cave. Both the observed and calculated anomalies have a magnitude of about -35 μGals. Although the cave was originally thought to be located near the center of the line, the observed gravity shows that it is located closer to the 20 ft position.

Rennie's Cave profile line strikes north to south, and crosses over the cave approximately 55 ft west of the cave mouth. The cave ceiling is estimated to be 5-10 ft beneath the ground surface at the profile line position. The cave is modeled as an irregularly shaped cylindrical feature, with the largest portion 8 ft wide. The air-filled cave is modeled to have a density contrast of -2.7 g/cc with the surrounding dolomite. Fig. 2-7 shows the observed and calculated gravity along the profile line. At the expected cave crossing, the observed and calculated anomalies match reasonably well, and have a magnitude of -50 μGals. North of the cave, there is a second observed anomaly that may be due to an unknown portion of the cave. However, this second anomaly may be an artifact of the terrain correction, since it is located at the base of a steep hill.

These two caves represent the largest caves expected within the Knox dolomite and the largest density contrast possible between bedrock and the cavity fill material. However, the small gravity anomalies due to both of these caves could easily go undetected if transected by the nominal station spacing of 50 ft used over most of the profile lines in this study. Since most of the cavities within the K-25 Site are expected to be smaller than the caves and filled with water and mud, it is unlikely that the gravity profiles are useful in detecting single cavities. It is more realistic to expect the gravity profiles to detect concentrated areas of cavities, where the sum effect of all the cavities produces a significant gravity anomaly.

## 2.6 DATA QUALITY ASSURANCE

During a gravity survey, factors that act to degrade the accuracy of the data include rough meter handling, a vibrationally noisy station location, elevation errors, instrument drift errors, and improper operation of the instrument. Since the detectability of the targets of interest is directly affected by the data accuracy, the survey was conducted using techniques to minimize all possible errors. Standard field procedures outlined in the L&R instruction manual (L&R 1991) were followed throughout the survey.

After each shipment of the gravity meter and periodically throughout the survey, the meter's electronic levels and sensitivity were adjusted to the specifications given by the L&R instruction manual (L&R 1991). On May 10, 1995, the meter was not functioning properly, and was returned to J. D. Fett

# COPPER RIDGE CAVE

**BRUNTON AND TAPE SURVEY (TRN21)**

*Paul A. Rubin, Bruce Zerr, Gareth Davies*

***Low Flow Conditions 12/19/92***

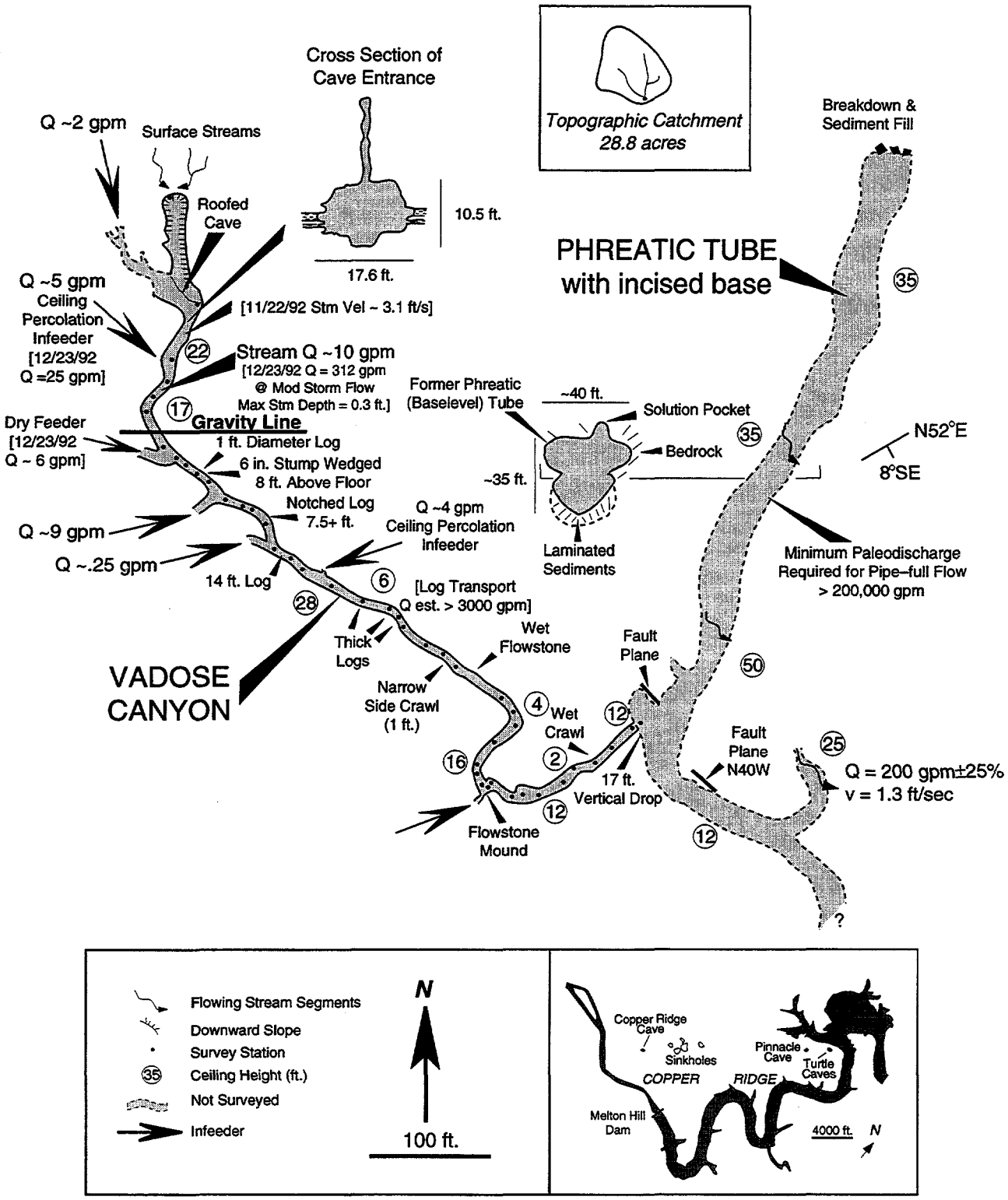


**Fig. 2-4. Map of Copper Ridge Cave showing the approximate location of the gravity profile line.**

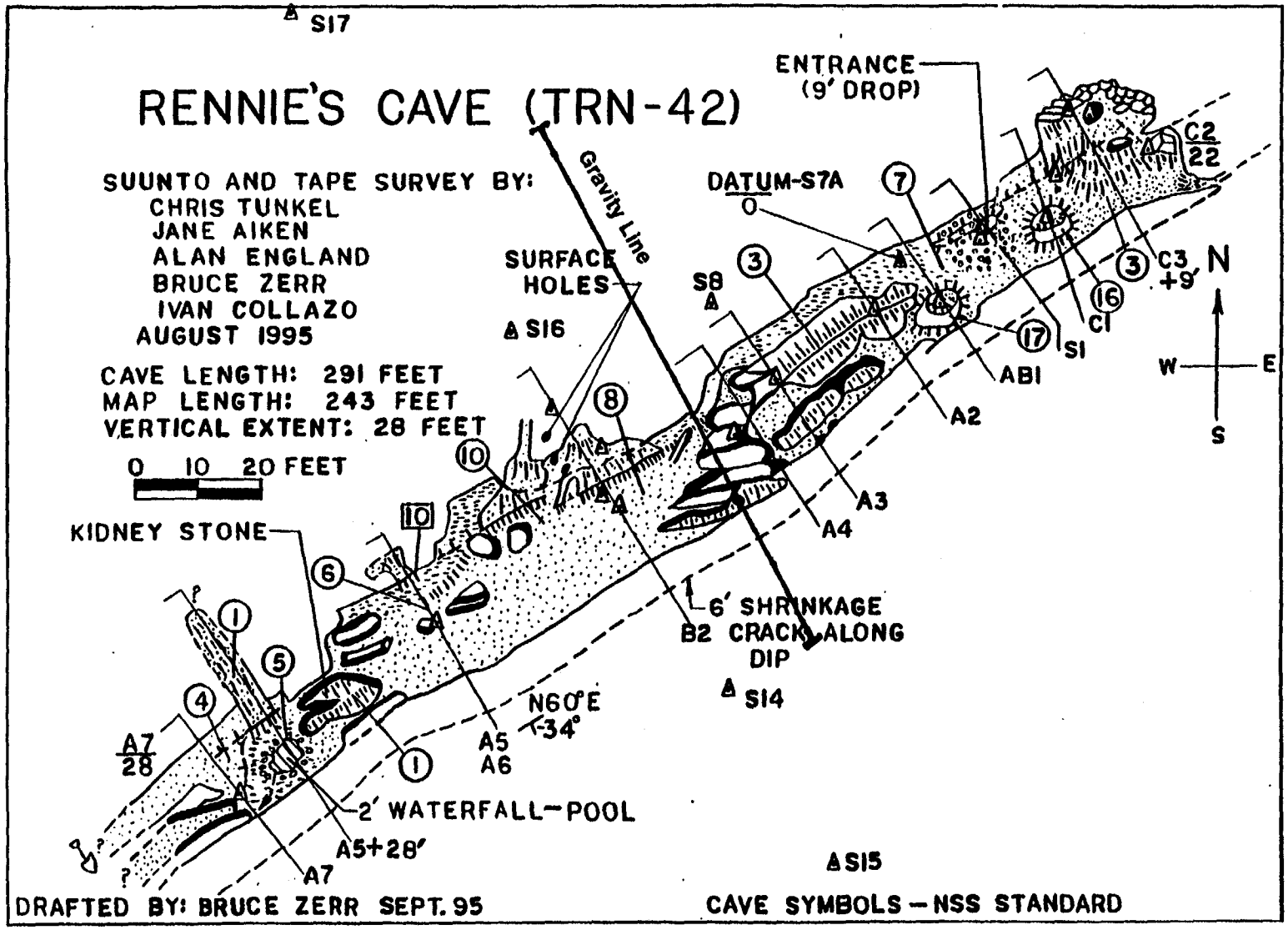


Fig. 2-5. Map of Rennie's Cave showing the approximate location of the gravity profile line.

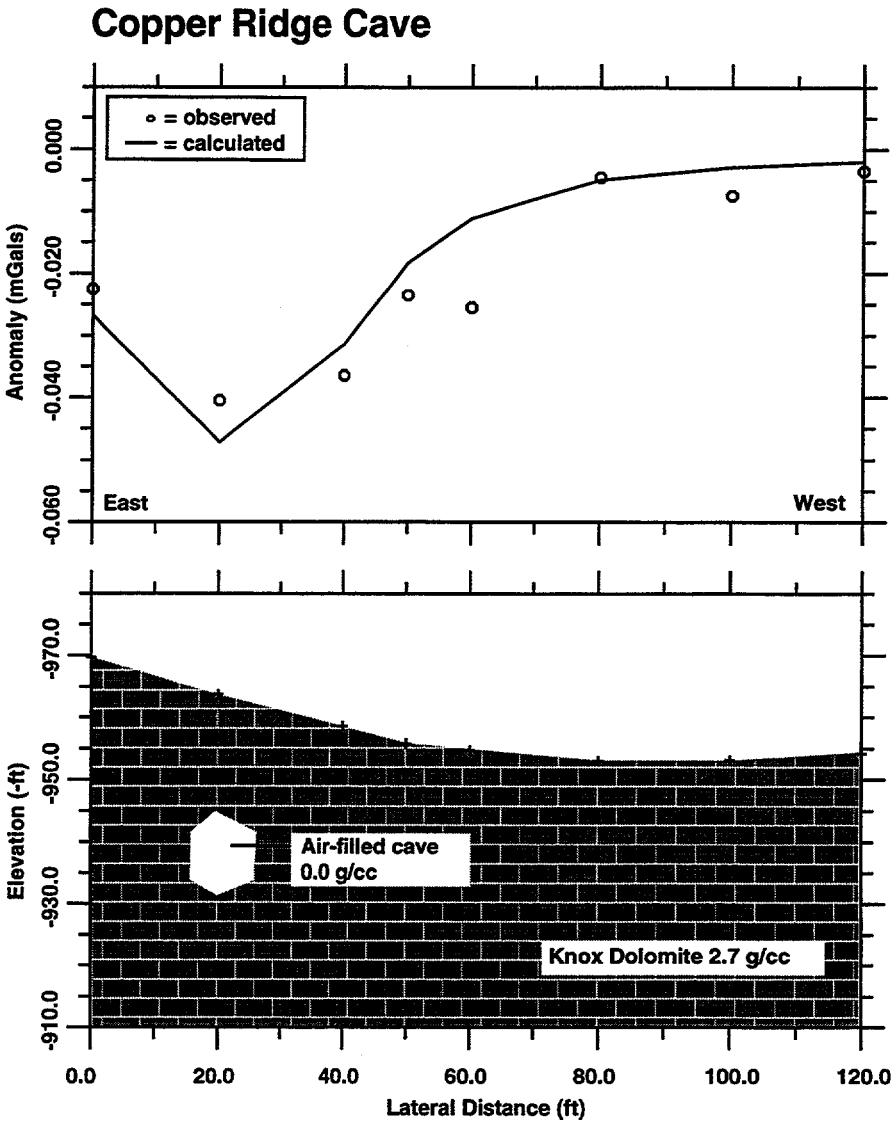


**Fig. 2-6. Model of Copper Ridge Cave gravity profile.**

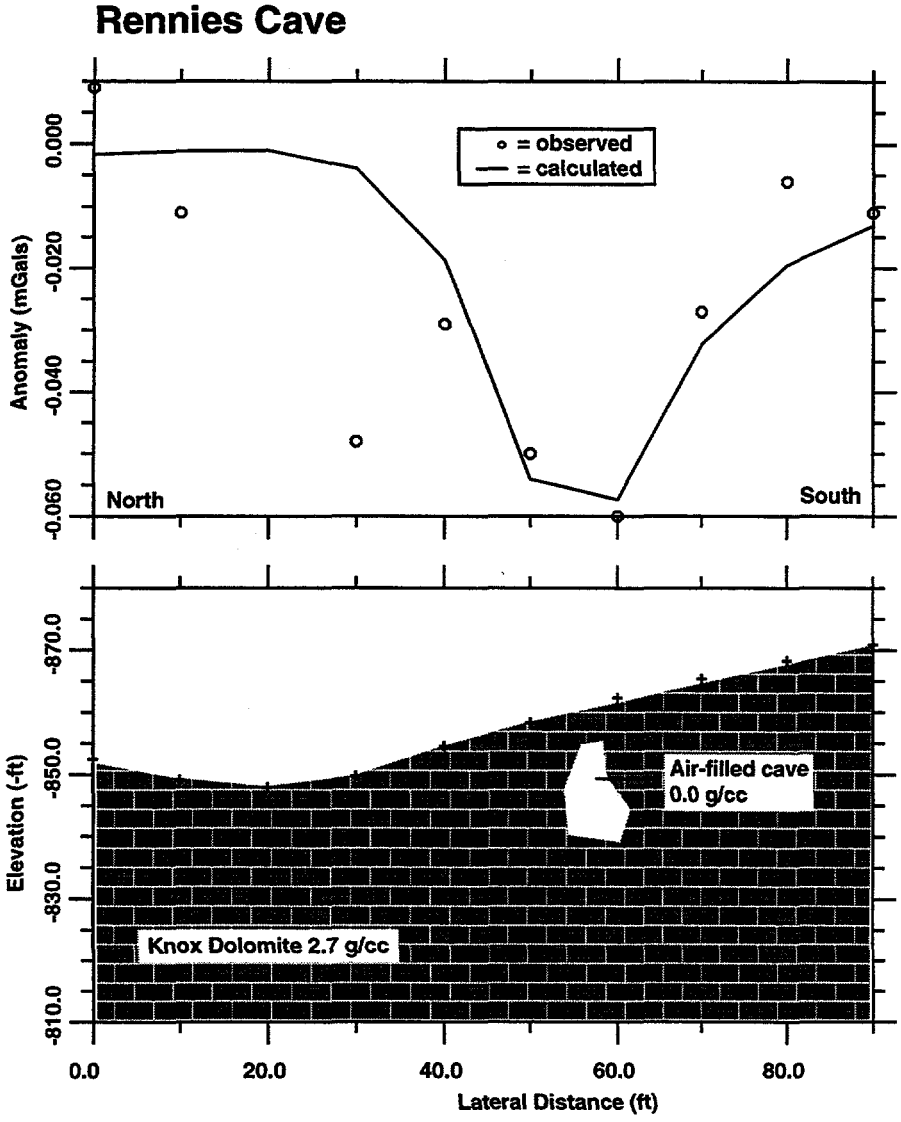


**Fig. 2-7. Model of Rennie's Cave gravity profile.**

Instruments, Inc. for repair. At all other times, the meter operated within the calibration limits set by the manufacturer.

Barge, Waggoner, Sumner, and Cannon, Inc. surveyed the positions and elevations of stations with a precision of 0.01 ft. Wells and catch basins that were previously surveyed provided additional measurement points. The elevation of the gravity meter above the survey stakes was measured using a ruler. Assuming a maximum 0.1 ft elevation error, the maximum effect on the simple Bouguer gravity due to the elevation error is approximately 6 μGals.

The meter was transported in its padded aluminum carrying case at all times to minimize the vibrations to the instrument. Frequent base station occupations (at least once per hour) corrected for the linear drift of the instrument. However, sporadic vibrations and occasional nonlinear drift of the instrument did produce error that could not be removed from the data. The data were acquired in pseudo-random order to minimize the effects of any systematic errors that may have occurred.

The repeatability of the base station readings were checked daily to confirm that the meter was operating correctly. After acquiring data each day, the field readings were reduced to simple Bouguer values and potential erroneous readings were identified. Approximately 21% of the stations were reoccupied to provide data confidence and repeatability. The average difference between the original and repeated readings is 8.4 μGals, which is within the expected resolution of the L&R model D microgravimeter under field conditions.

## 2.7 DATA ACQUISITION

The locations of the gravity measurement stations in the ORNL administrative grid system are shown in Fig. 2-8. Four north-to-south profile lines were surveyed that are oriented perpendicular to local geologic strike at various locations within the K-25 area. These lines are labeled as lines 1, 2, 3, and 10. The lines have a station spacing of 50 ft, and portions of line 1 have a spacing of 25 ft. In addition, stations were added within the K-901 area in order to fill areas of sparse data coverage from microgravity surveys performed in 1992 by Environmental Consulting Engineers, Inc. and in 1994 by Blackhawk Geosciences. The data from the previous surveys of the K-901 area are included in this report, and integrated into a new analysis of the K-901 area.

Wells and catch basins scattered around the K-25 plant were previously surveyed for their position and elevation, and served as convenient, additional gravity stations for the study. The catch basin stations form additional lines labeled 5, 6, 7, 8, 9, and 11. The catch basin station spacings vary, but typically range from 50-100 ft.

All measurements are tied to an absolute gravity base station outside of the geology building at the University of Tennessee. This station has an absolute gravity value of 979,697.14 mGals. The exact location of this and the other field base stations are reported in Appendix A. Future gravity surveys of the area may be tied with the data from this study by simply reoccupying one of these base stations.

A base station located in building 3504 at ORNL was occupied at least twice each day, and the field base stations were occupied at least once each hour during data collection to account for instrument drift. The acquisition time for each station varied between 5 and 20 minutes depending on the site conditions. Hard concrete allowed fast instrument leveling, while soft, irregular ground slowed the leveling process. The date, time, meter height, and gravity reading at each station were recorded in a log book and later transferred to a computer for processing.

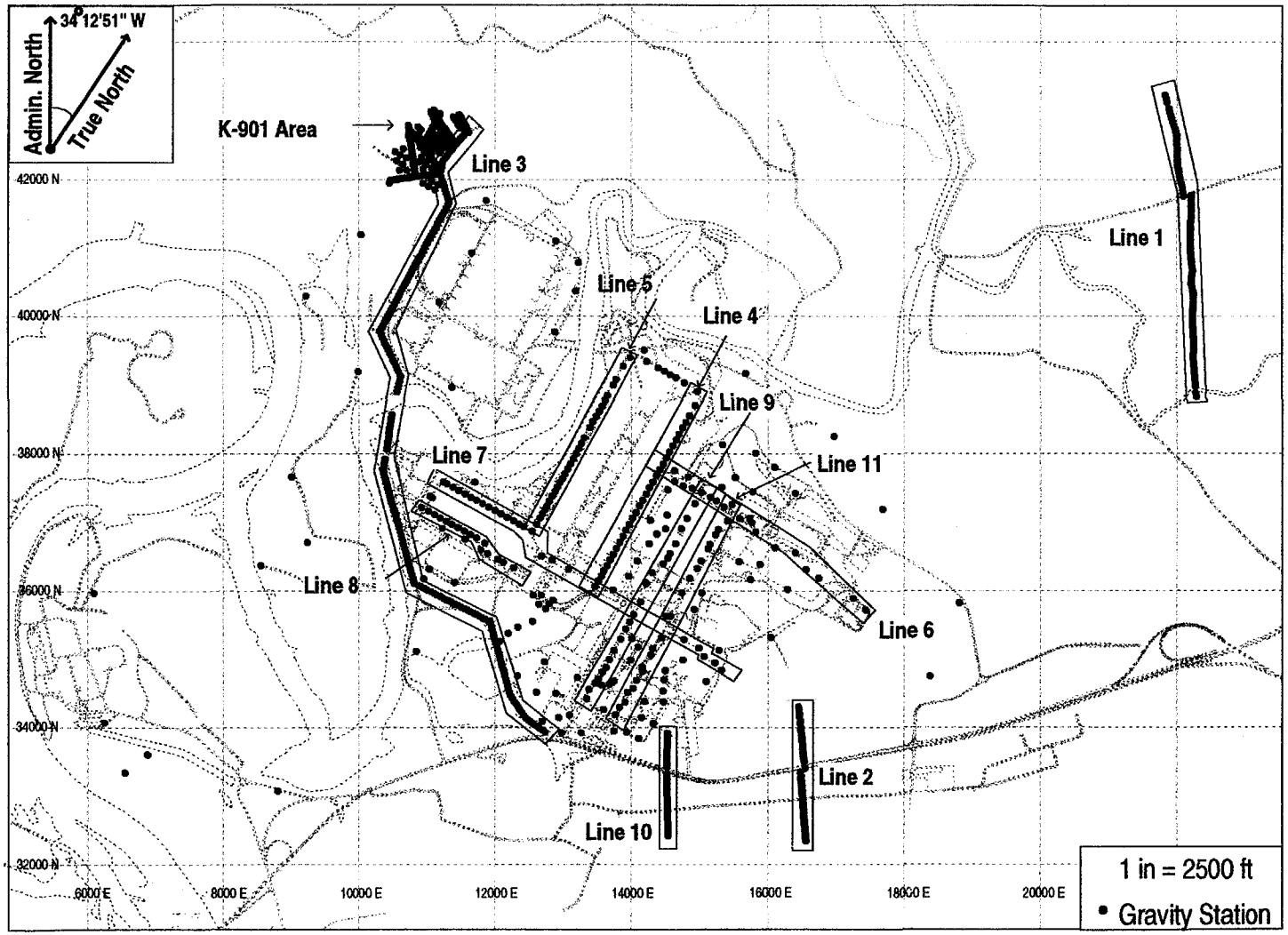


**Fig. 2-8. Locations of the gravity stations and the profile lines.**

## 2.8 DATA REDUCTION

The raw data were reduced to simple Bouguer values using GRAVPAC (L&R) software on an IBM-compatible computer. This processing step was performed regularly during the data acquisition to ensure data quality. Measurements along each profile line that were discontinuous with the rest of the profile were identified and reacquired.

A terrain correction was applied to the simple Bouguer values using digital elevation maps of the K-25 area and a computer program developed by Environmental Consulting Engineers, Inc. The computer program was tested and proven reliable by comparing its results with those obtained by calculating the terrain correction with a standard formula presented in Telford et al. (1976). The terrain correction corrects for the upward gravitational attraction of nearby hills and the lack of downward gravitational attraction caused by the missing mass of nearby valleys. Since much of the data was acquired on or near ridges, the terrain correction proved to be a significant factor in the data reduction.

The terrain correction accounts for topography within a specified area surrounding each station. The correction is significant if the ratio of the elevation change to lateral distance from the station is greater than approximately 1/20. Based on the topography within the K-25 study area, a circular area with a radius of 3000 ft from each station will account for all significant terrain effects. This area was divided into a set of concentric circles and radial lines that form sectors of increasing area from the center. Using the Hammer (1939) method, the computer program calculated the average elevation and gravitational influence of each sector. The sum of the gravitational effects of the sectors was added to the simple Bouguer gravity value at each station.

Digital elevation maps of the plant provided the elevations used in the terrain correction (Coleman et al., in preparation). All of the stations, except those in line 1, were corrected with the 1992 K-25 elevation map digitized on a spatial grid of 25 ft centers. Line 1 is outside the 1992 map coverage, so the Oak Ridge Reservation map digitized on a spatial grid of 100 ft centers was used for the terrain correction of line 1. Smaller elevation grid spacings will more accurately account for the terrain effects due to small features such as ditches and boulders, but increase the computational time necessary to calculate the effects.

The simple Bouguer and terrain corrections combine to remove the effects of topography from the gravity data. An appropriate density (referred to as Bouguer density) must be chosen for these corrections that approximates the density of the material between the station and datum. A Bouguer density that is too low will under-correct the topographic effects and leave the data correlated with topography, while a Bouguer density that is too high will over-correct the topographic effects and leave the data anti-correlated with topography. Fig. 2-9 illustrates these effects showing the complete Bouguer gravity for line 2 using various density values. A Bouguer density value was chosen separately for each profile line that produced the least correlation with topography (e.g. 2.1 g/cc for line 2). Since the profile lines are located over different lithologic units, different Bouguer density values can be expected. These Bouguer density values were used in the analysis of the individual lines; however, a Bouguer density of 2.4 g/cc was used when the data were combined into a contour map.

## 2.9 CULTURAL EFFECTS

Man-made objects, such as buildings and catch basins, will have an effect on the gravity measurements if located too close to the station. It is difficult to account for these effects, unless accurate

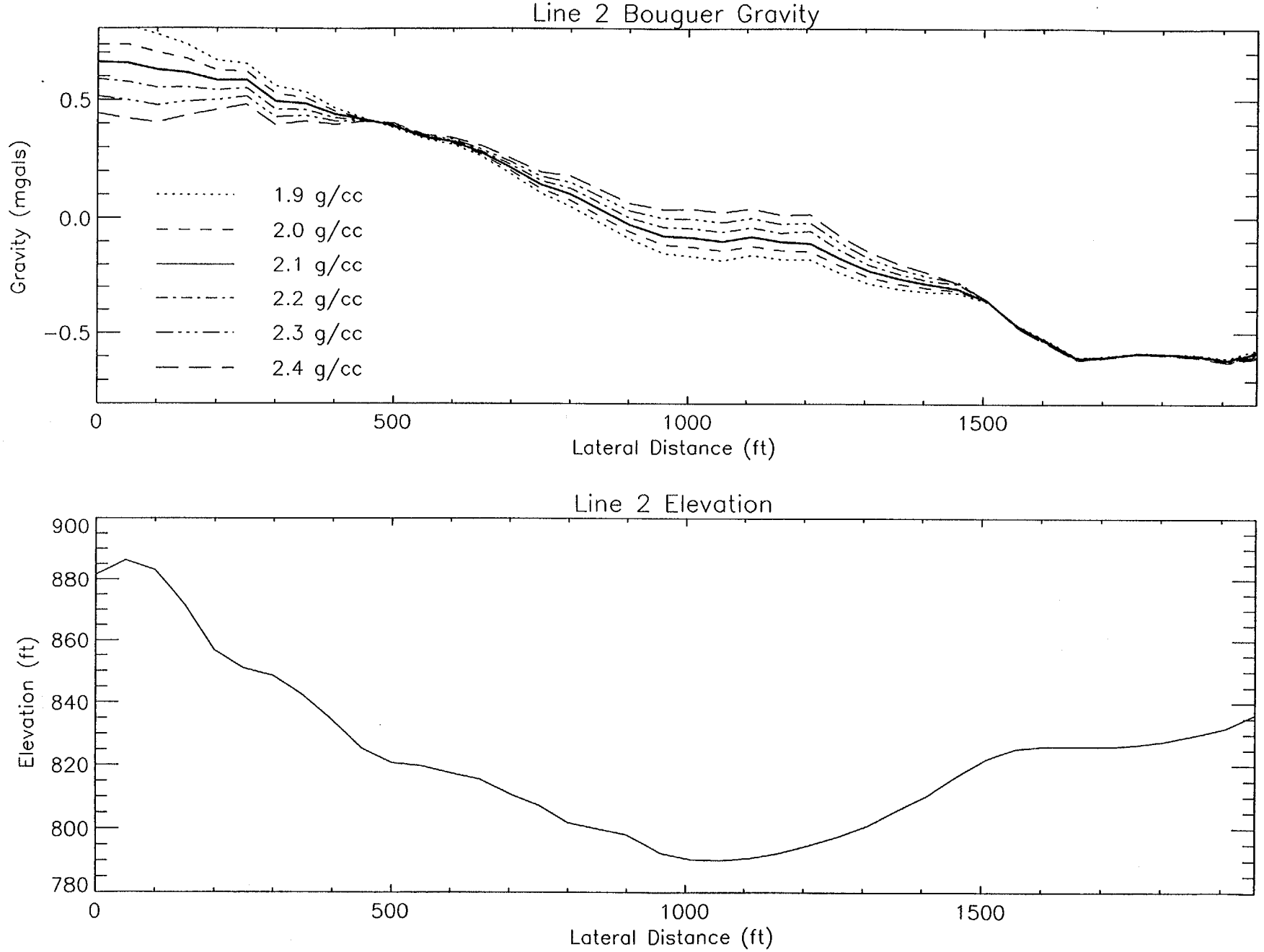


**Fig. 2-9. Terrain corrected gravity and elevation profiles of line 2. The gravity is calculated with a range of Bouguer densities.**

size and density information can be obtained. The largest building in the area is the K-25 building, which lies close to lines 4, 5, 6, and 7. No obvious effects from the building are seen in the data from these lines, since the values closest to the building are continuous with those further from the building. A simple forward model of the gravitational effects of the building may be obtained by assuming a density contrast, and calculating the terrain correction.

Fig. 2-10 shows the terrain correction as a function of distance from the building's wall. The model assumes a building material density of 4.0 g/cc, which represents an estimate of the combined bulk density of concrete, metal, and wood used to construct the building. The effects of three different percentages of material occupying the building's volume are presented. The models indicate that a 20% material volume would require a terrain correction of >50 μGals for stations within 50 ft of the building. Since most of the gravity stations are further than 50 ft from the building, the greatest effects due to the building are assumed to be less than 50 μGals. Although 50 μGals is above the detection threshold, an accurate correction for the building effects could not be accomplished without obtaining detailed dimensions and densities of the building and objects within the building.

Some of the stations within the plant are located on grates above catch basins. The catch basins are drainage holes with lateral dimensions that average 3 × 3 ft and depths that range from 0-25 ft. The gravitational effects of each of the catch basins were calculated by assuming the basins are vertical cylinders having a radius of 1.5 ft. Measured depths of each catch basin and a density contrast corresponding to missing regolith (1.9 g/cc) were used in the calculation. The effect ranged from 0-36 μGals with an average of 30 μGals. These values were added to the data from the catch basin stations to correct for the missing mass beneath the catch basin grates.

## 2.10 REGIONAL REMOVAL

In order to interpret anomalies due to small-scale features, any regional trends must be removed from the data. The Bouguer Gravity Anomaly Map of Tennessee (Johnson and Stearns 1967) contains a southeast trending gravity gradient in eastern Tennessee, including the Oak Ridge area. Watkins (1964) discusses the gradient in eastern Tennessee and the importance of removing it before interpreting gravity anomalies. The gradient is continuous regardless of the local geology or topography and has a value of approximately -0.5 μGals/ft SE in the vicinity of K-25.

Data obtained in this study show the dominating effect of the regional gradient (Fig. 2-11). To remove the effect of the regional gradient, a planar surface was fit to the data using a least squares polynomial regression. The data set was evenly sampled in the gradient calculation to equally weight measurements from all portions of the study area. In the K-25 grid system, the plane equation is:

$$g_p = -0.31x + 0.50y$$

where x and y are the easting (ft) and northing (ft) coordinates respectively, and $g_p$ is in μGals. Therefore, the magnitude of the gradient is approximately -0.59 μGals/ft in the K-25 grid direction of S32E. The value agrees with the gradient estimated from the state map, and remains constant when only subsets of the data are used in the plane calculation. Also, the value is independent of the assumed Bouguer density, which indicates that the regional gradient is related to a deep crustal feature.

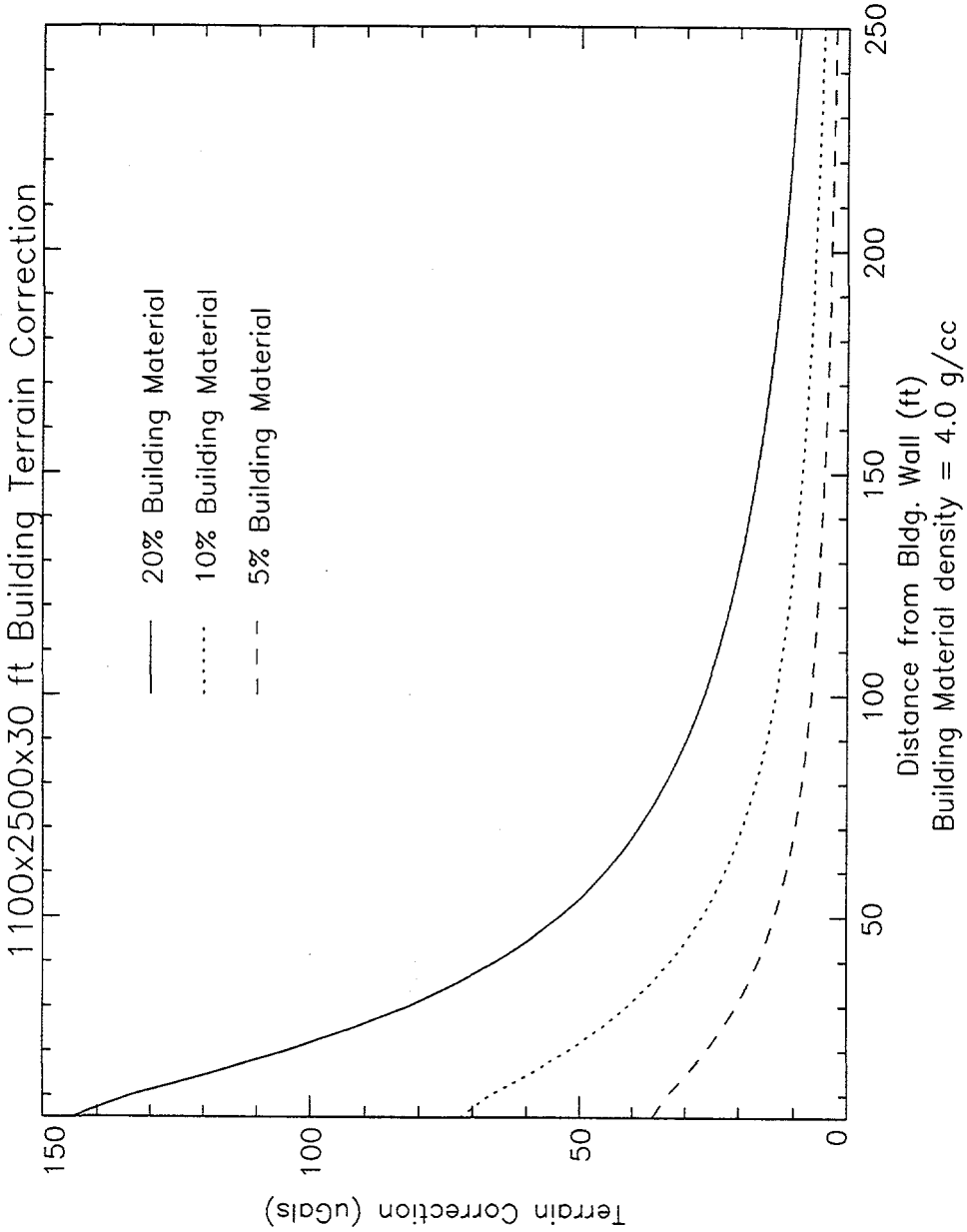


**Fig. 2-10. Modeled gravity effects of the K-25 Building as a function of distance from the building wall and percentage of volume occupied by building materials.**

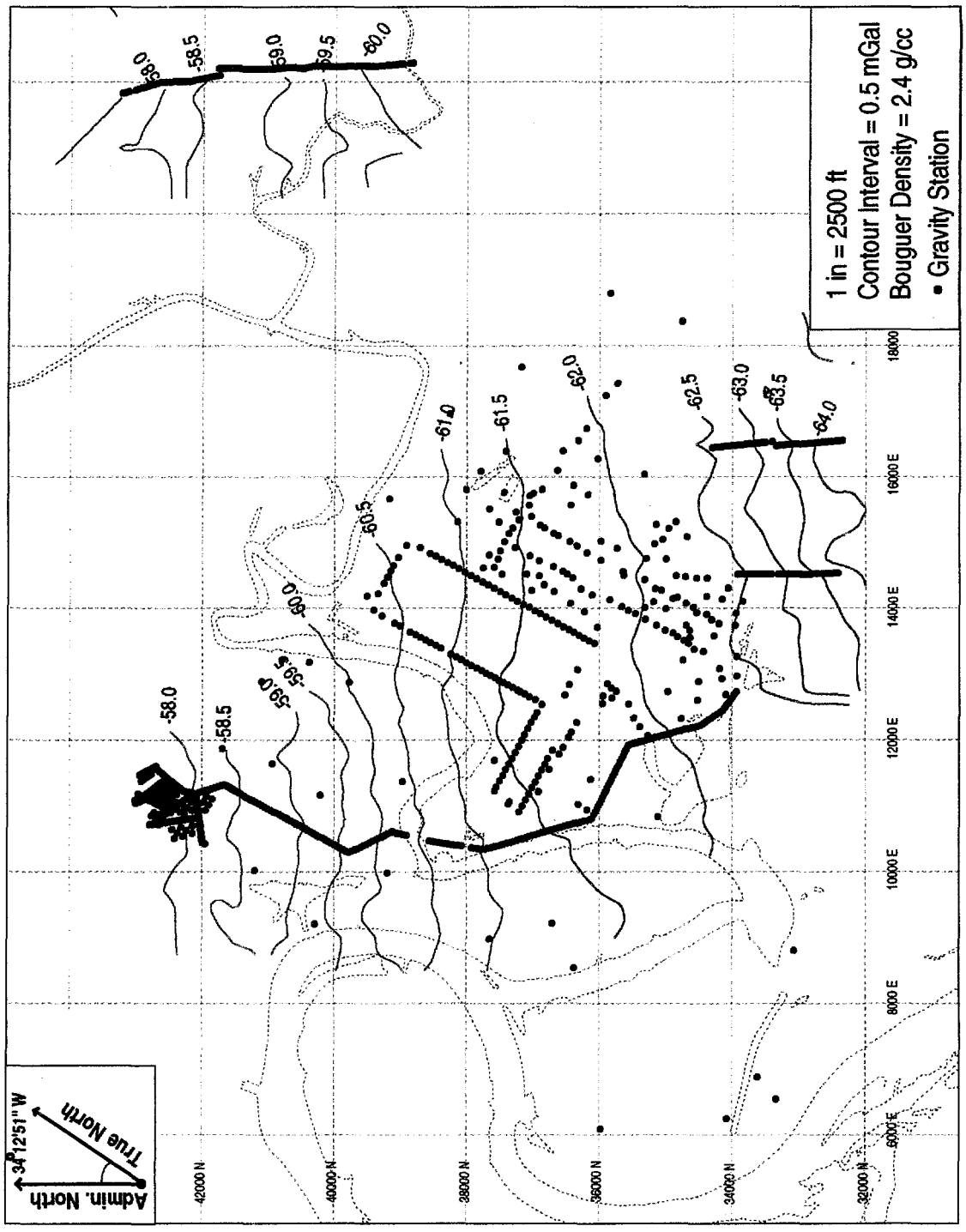


**Fig. 2-11. Contour map of the complete Bouguer gravity (density = 2.4 g/cc) for the K-25 Site. The regional gradient has not been removed from the data.**

# 3. GRAVITY DATA

The reduced, terrain-corrected gravity data are shown for each profile line in Figs. 3-1 through 3-11. The regional gradient and data set average are removed from the profile lines. Except for obviously bad measurements, all observed values for each point are presented in order to give an indication of the scatter in the data. The gravity profiles are annotated to show the most recent mapped surface locations of the stratigraphic contacts, faults, the syncline axis, and the anticline axis (Lemiszki 1994). Below each gravity profile, the elevation is shown along with the location of major surface features such as buildings and roads. A complete list of the simple Bouguer values, terrain corrections, and regional-corrected Bouguer values for all of the stations is available in the OREIS data base.

The data from the profile lines along with data points scattered throughout K-25 were gridded to produce a contour map (Fig. 3-12) that is discussed in detail in Chap. 4. The map shows the relative Bouguer gravity across the study area using a Bouguer density of 2.4 g/cc. The Surfer (Golden Software, Inc. 1994) linear kriging routine using a 2000-ft octant search parameter grid the data into 100 × 100-ft cells. An anisotropy ratio of 1.6 was used to weight the data along the east-west axis more heavily than the north-south axis in the gridding routine. The ratio is based on the spatial continuity of the data analyzed by a geostatistical computer program (Pannatier 1996). The data are contoured at 100-μGal intervals with negative values shown in red and positive values shown in blue.

Data acquired in previous surveys of the K-901 area are tied to the data acquired in this study. This procedure consists of reoccupying several of the old survey stations and finding the static shift between the data sets. Since the relative gravity difference between stations remains constant over time, the static shift may be added to the old data and combined with the newly acquired data. The same regional gradient removed from the entire data set was removed from the K-901 data subset. The K-901 data were gridded into 50 × 50-ft cells to produce a contour map (Fig. 3-13) that is discussed in detail in Chap. 4. The gridding routine used linear kriging with a 400-ft octant search parameter and no anisotropy. The average value of the K-901 subset was removed to show the relative gravity highs and lows within the K-901 area. Since the average within the K-901 area is different than the entire data set average, the values are statically shifted by -85 μGals from the full data set.

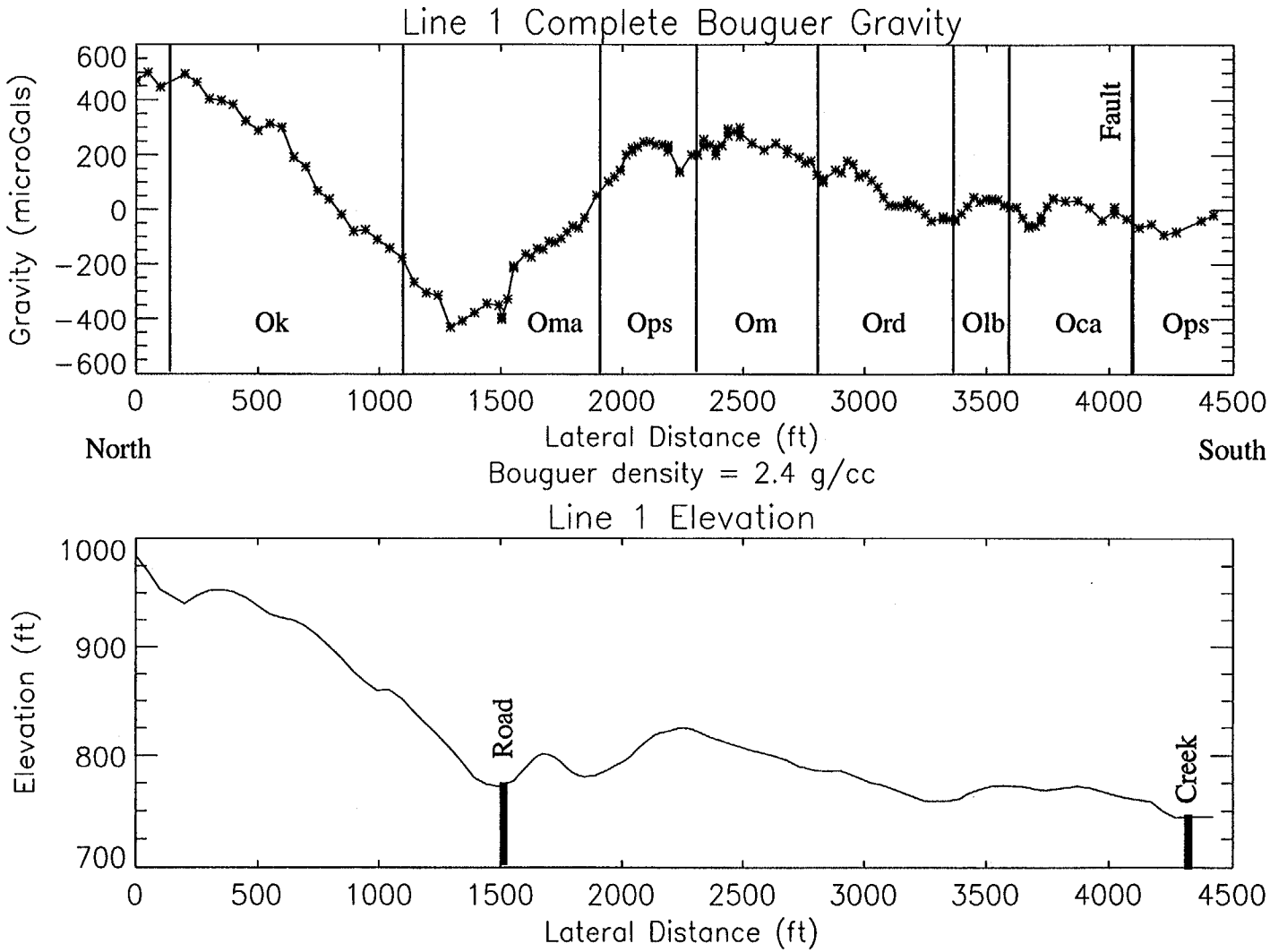


**Fig. 3-1. Complete Bouguer gravity and elevation profiles for line 1.**

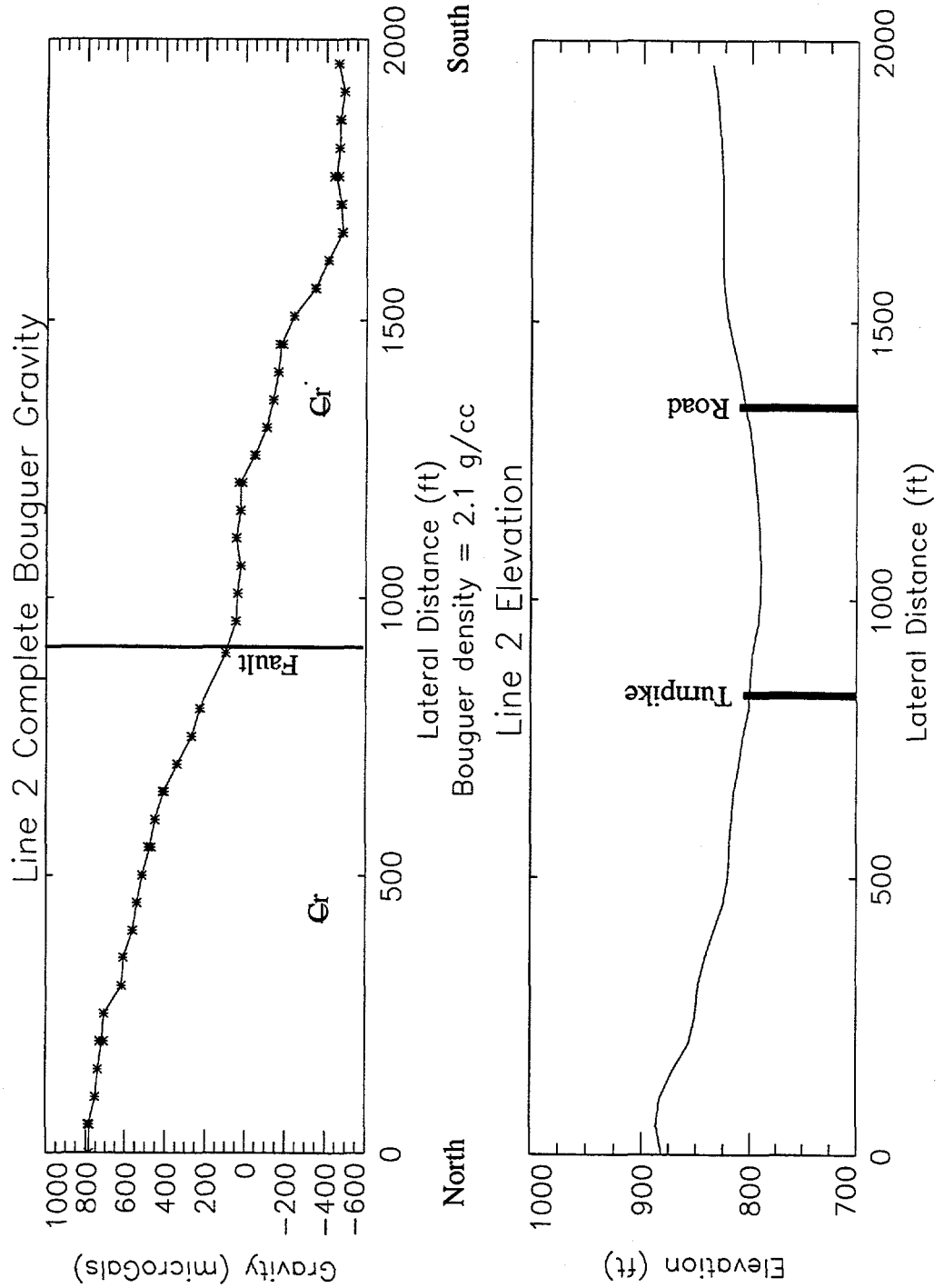


**Fig. 3-2. Complete Bouguer gravity and elevation profiles for line 2.**

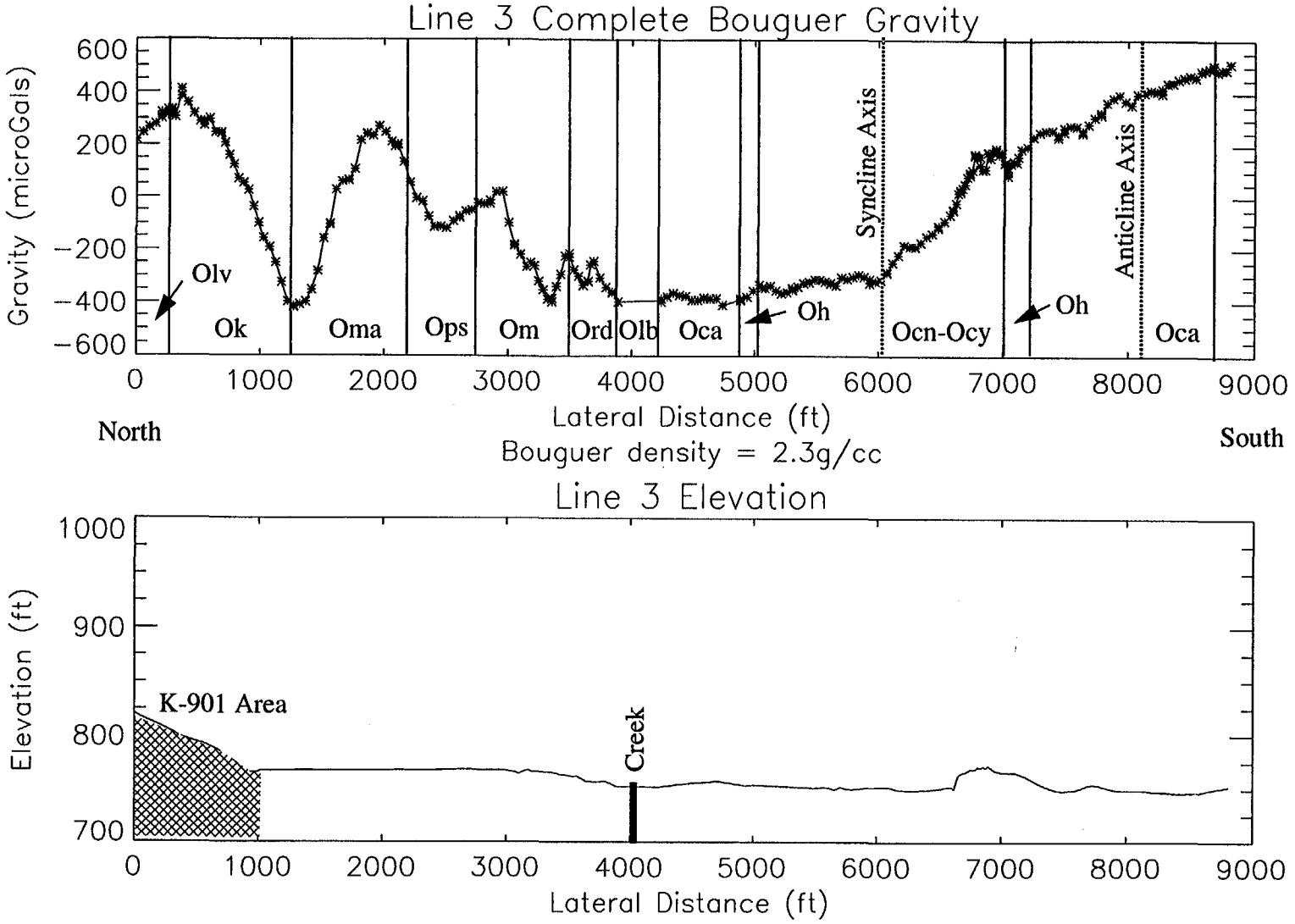


**Fig. 3-3. Complete Bouguer gravity and elevation profiles for line 3.**

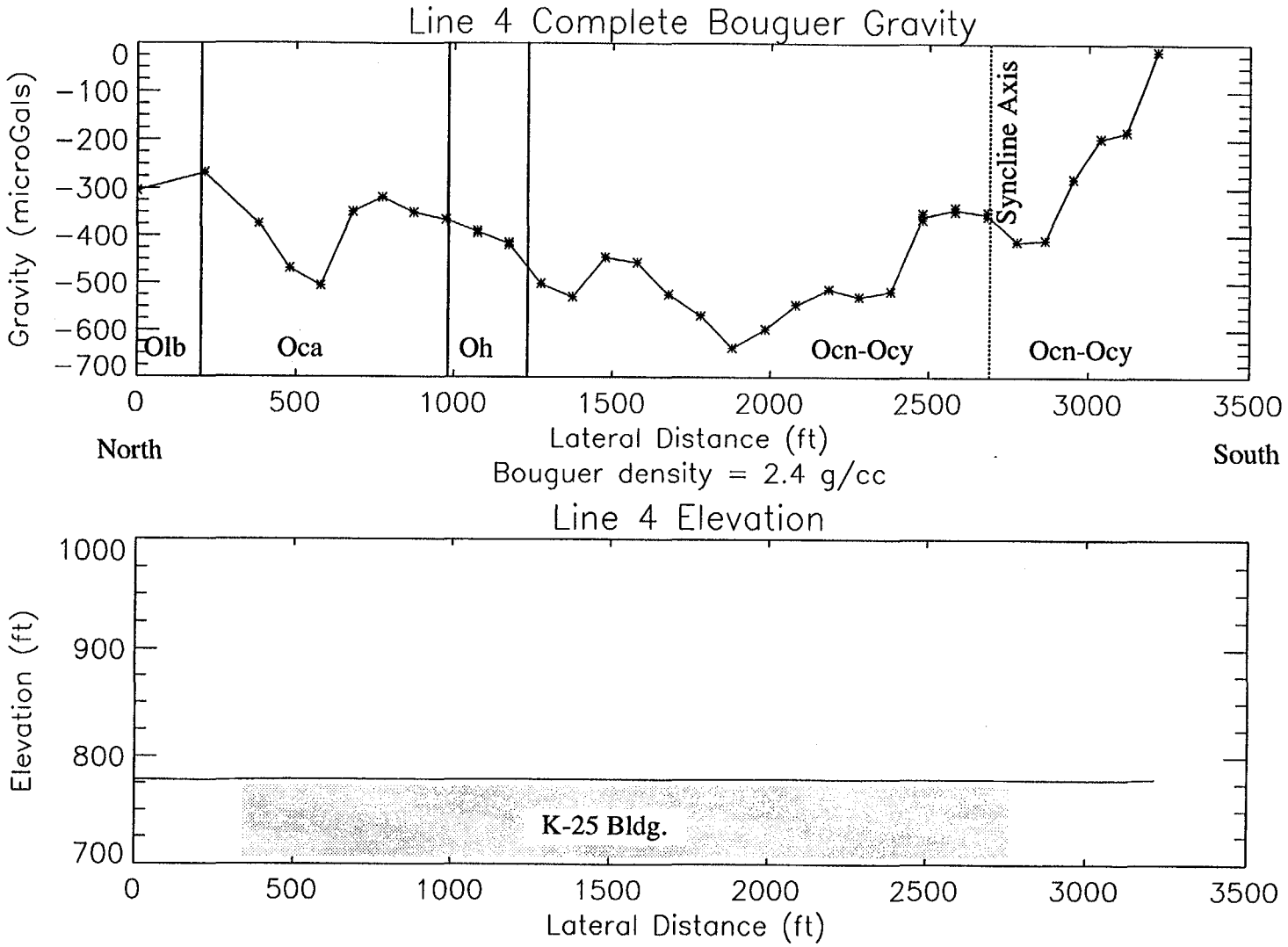


**Fig. 3-4. Complete Bouguer gravity and elevation profiles for line 4.**

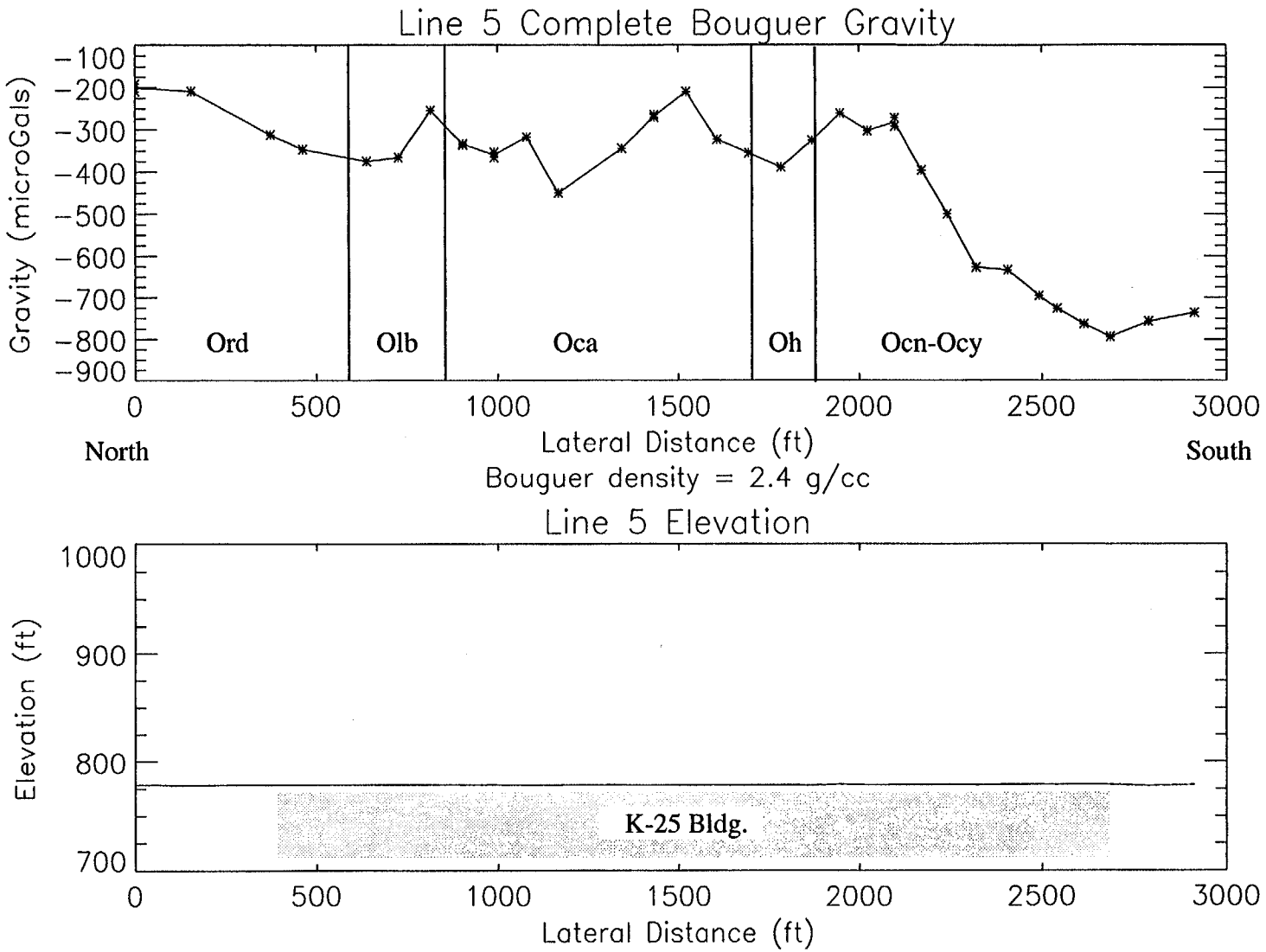


**Fig. 3-5. Complete Bouguer gravity and elevation profiles for line 5.**

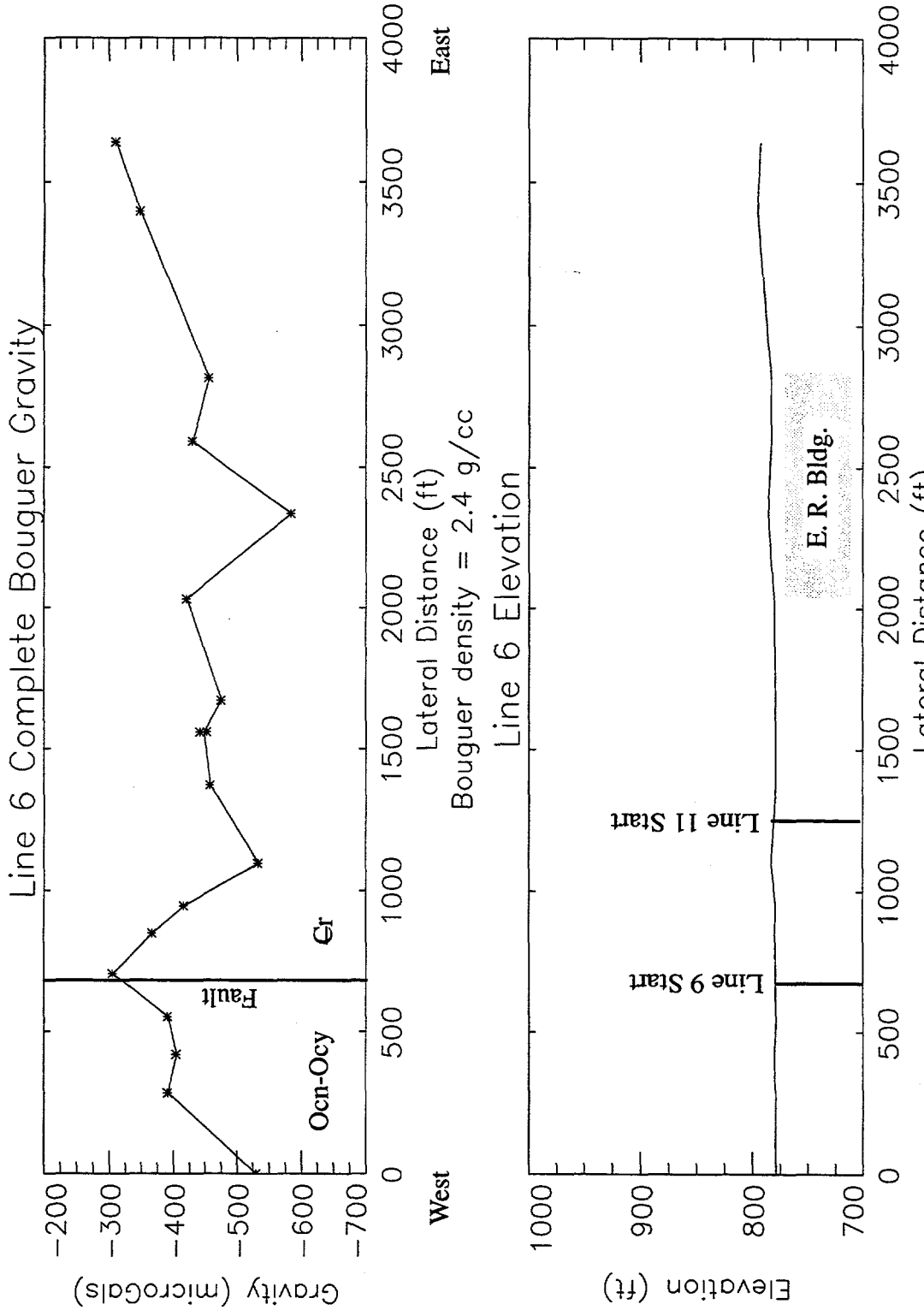


**Fig. 3-6. Complete Bouguer gravity and elevation profiles for line 6.**

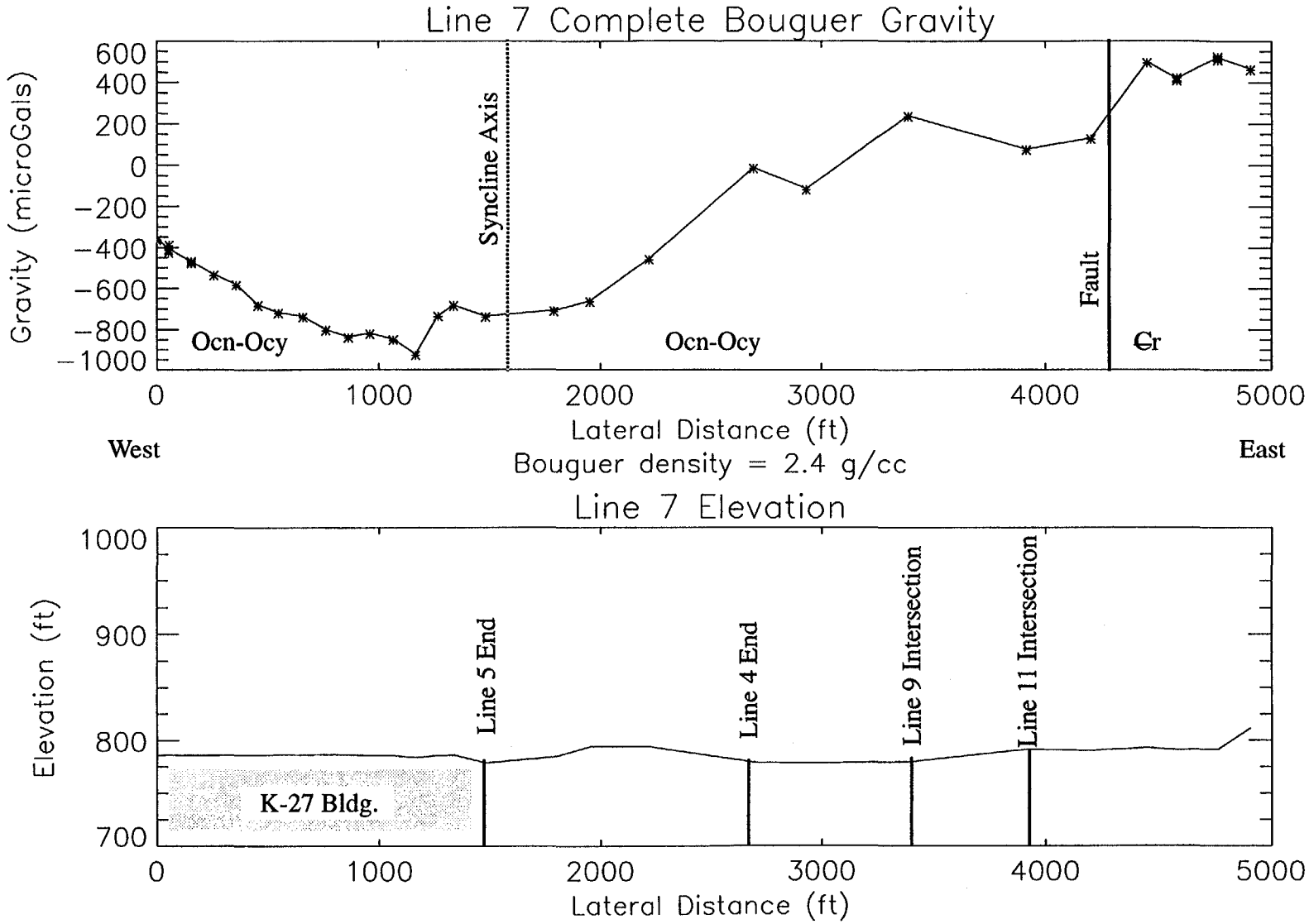


**Fig. 3-7. Complete Bouguer gravity and elevation profiles for line 7.**

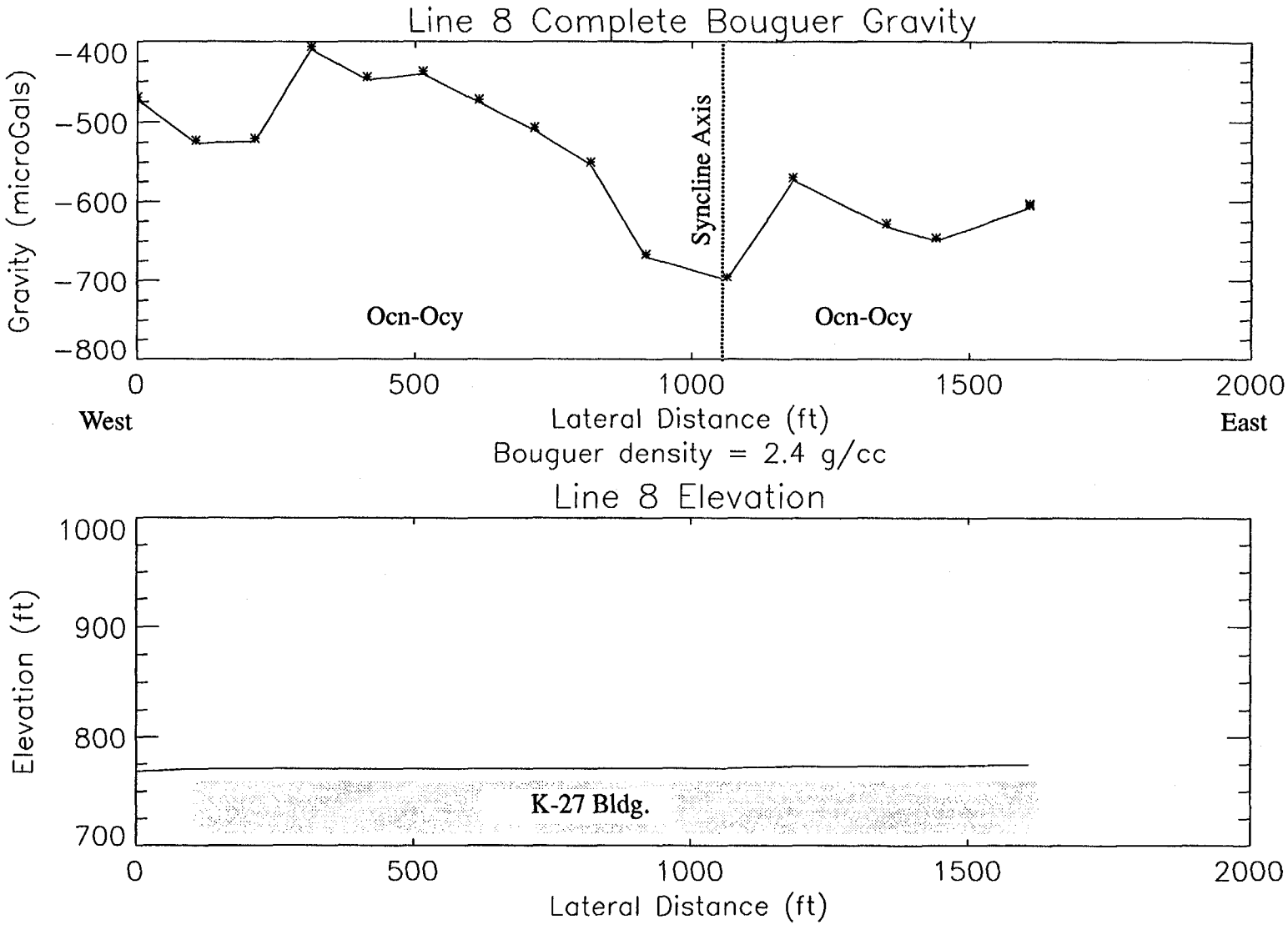


**Fig. 3-8. Complete Bouguer gravity and elevation profiles for line 8.**

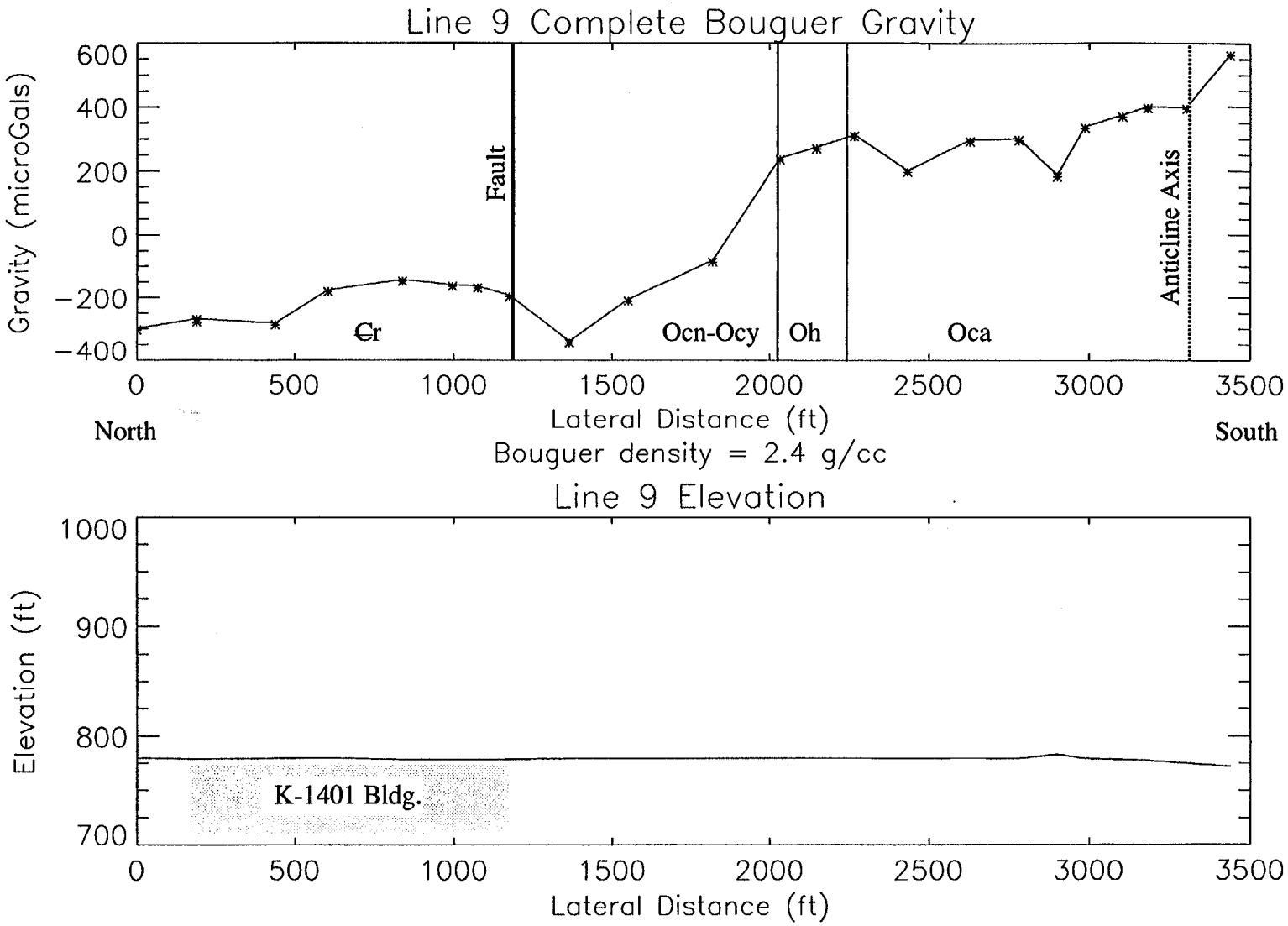


**Fig. 3-9. Complete Bouguer gravity and elevation profiles for line 9.**

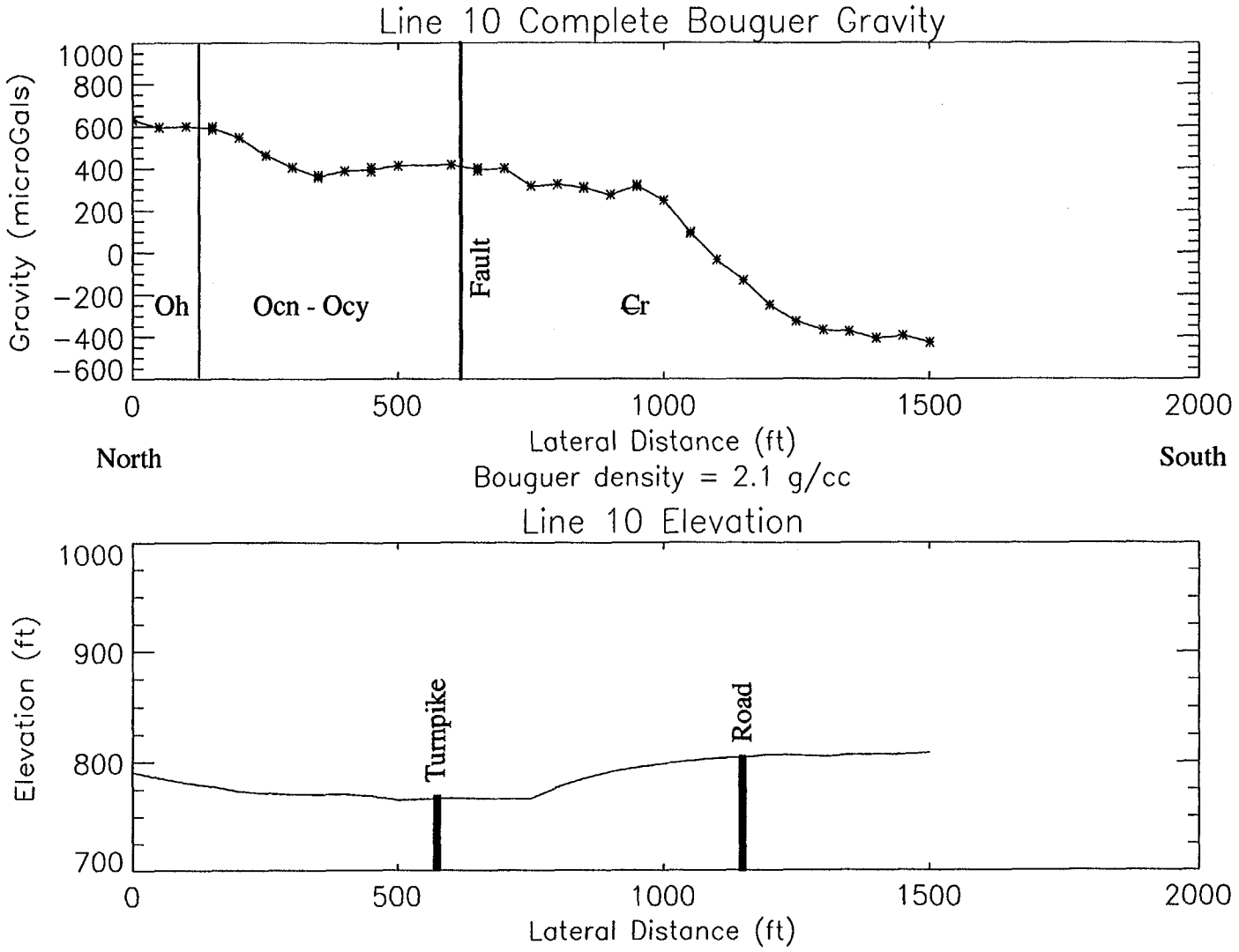


**Fig. 3-10. Complete Bouguer gravity and elevation profiles for line 10.**

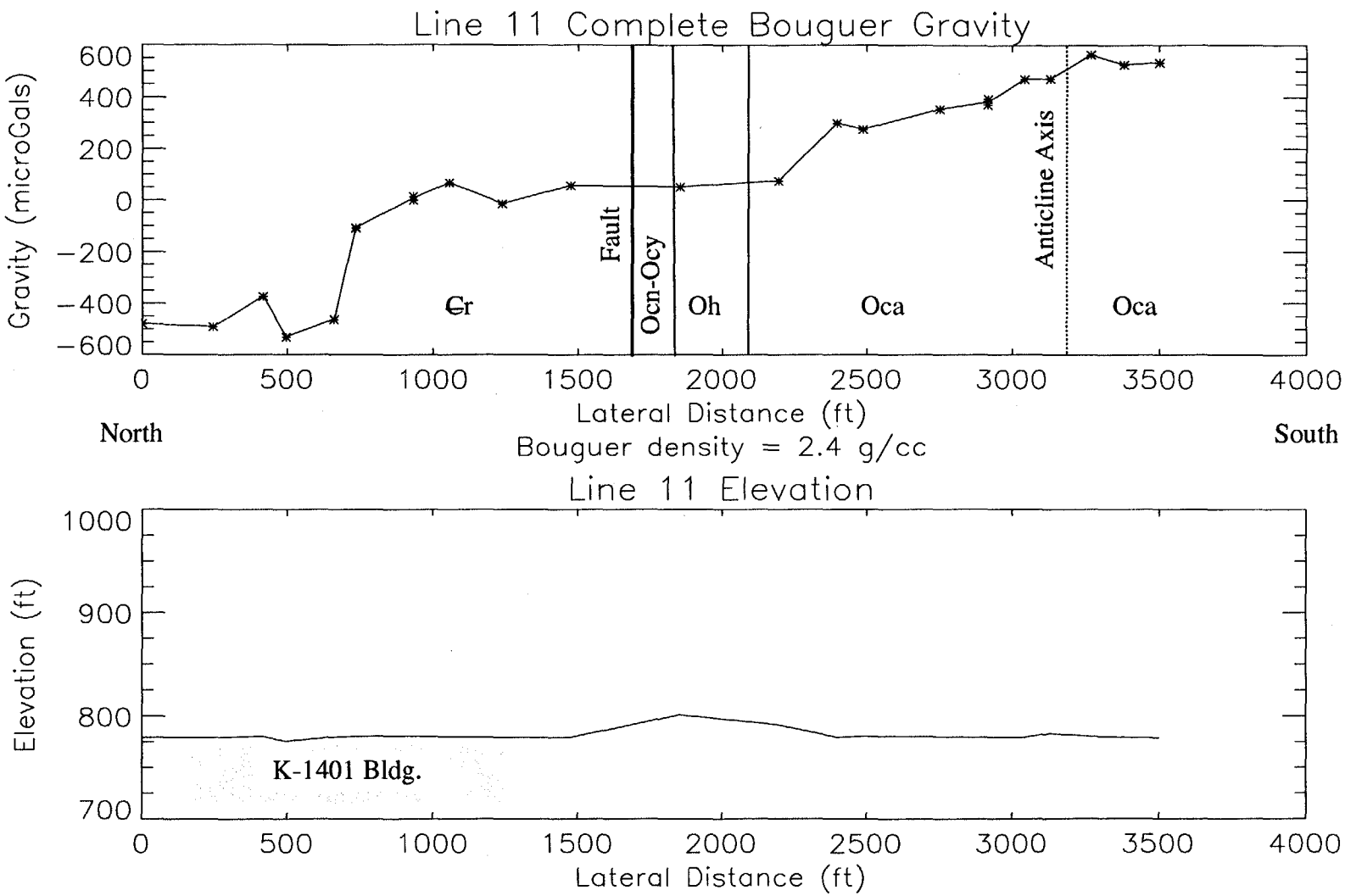


**Fig. 3-11. Complete Bouguer gravity and elevation profiles for line 11.**

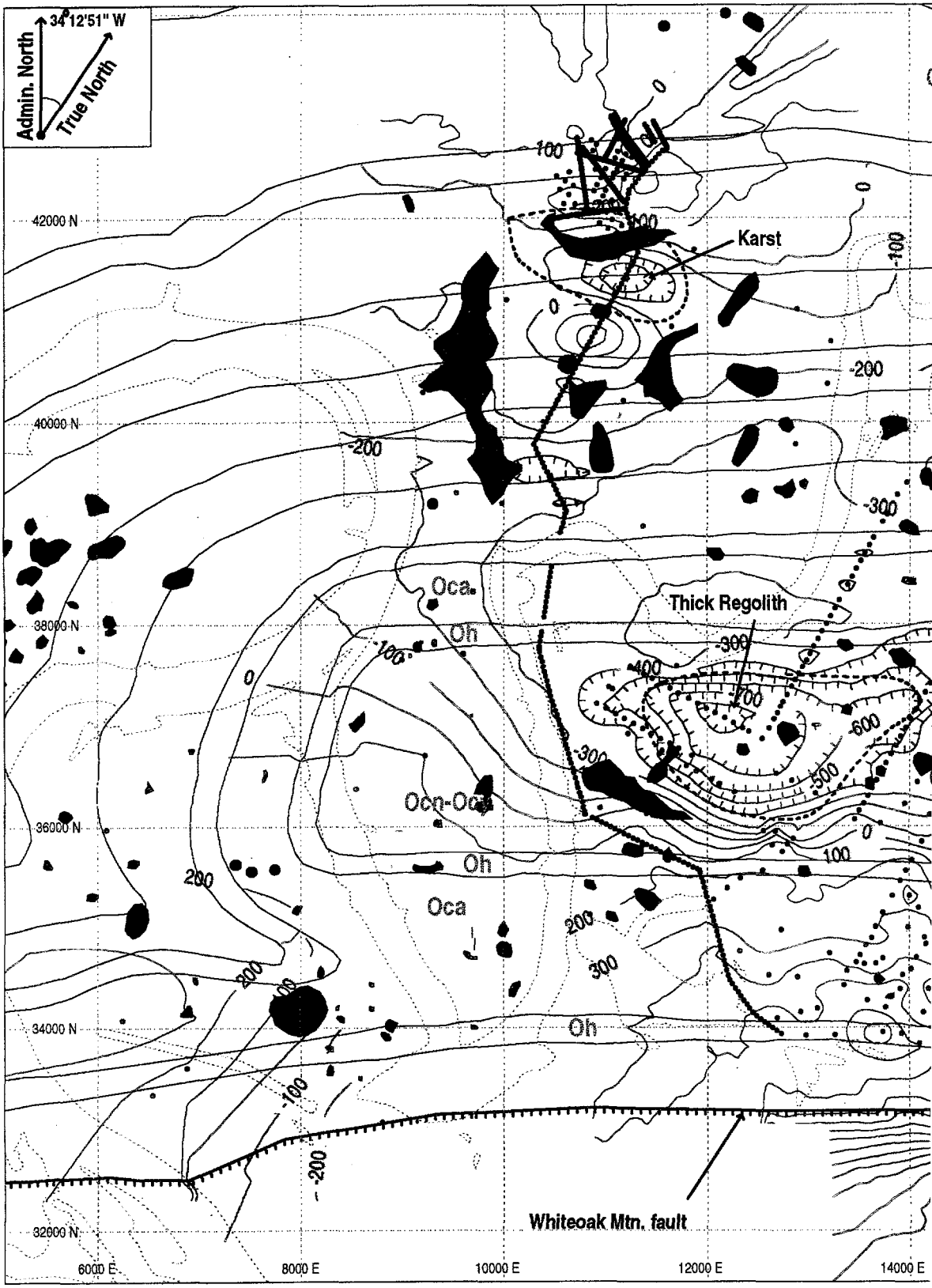
Admin. North
34°12'51" W
True North
42000 N
40000 N
38000 N
36000 N
34000 N
32000 N
6000 E
8000 E
10000 E
12000 E
14000 E
Karst
Thick Regolith
Whiteoak Mtn. fault
Oca
Oh
Ocn-Oca
0
100
200
300
400
500
600
700
-100
-200
-300

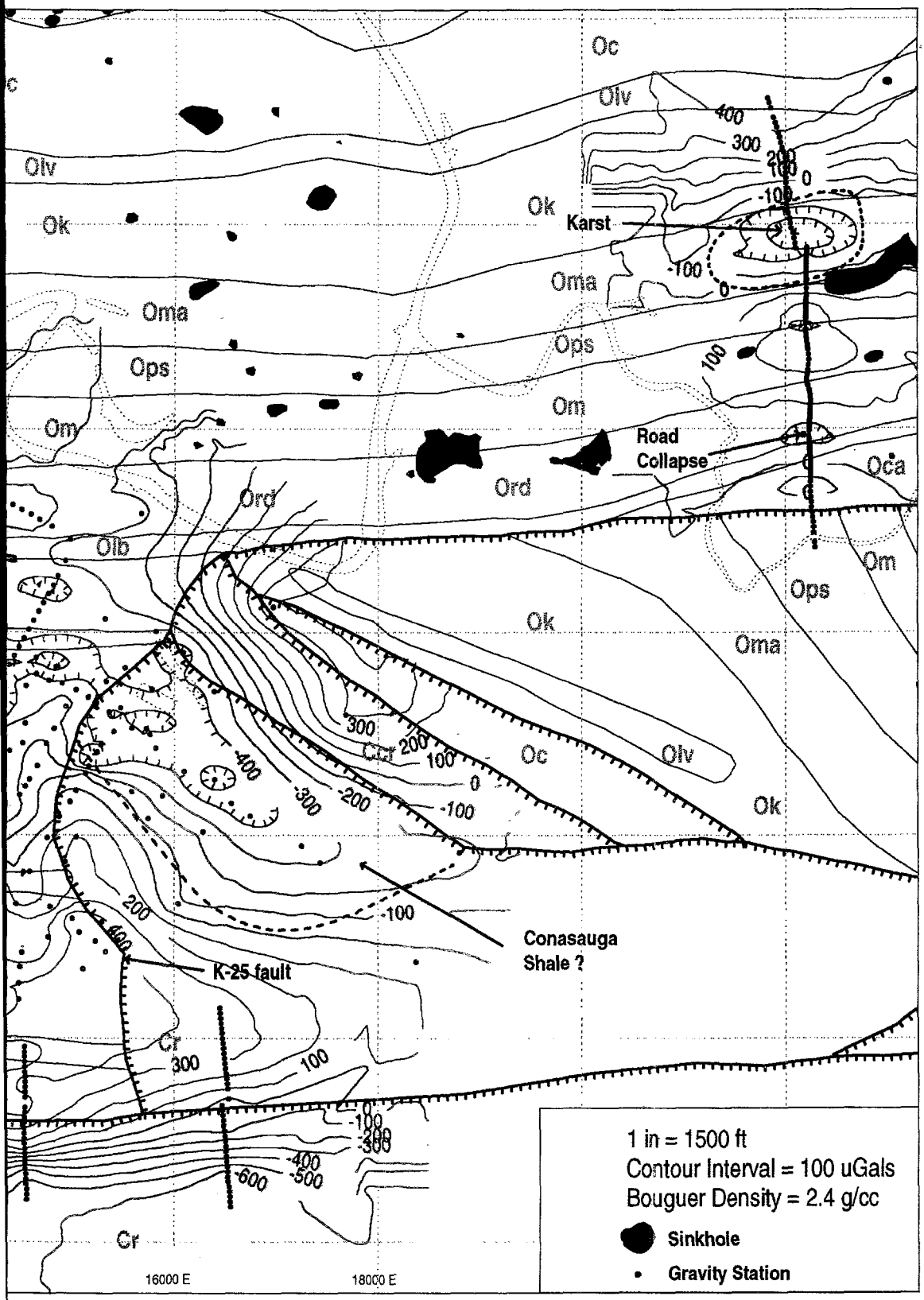


Fig. 3-12. Contour map of the complete Bouguer gravity for the K-25 Site with the regional gradient and data set average removed. Negative values are shown in red, and positive values are shown in blue.

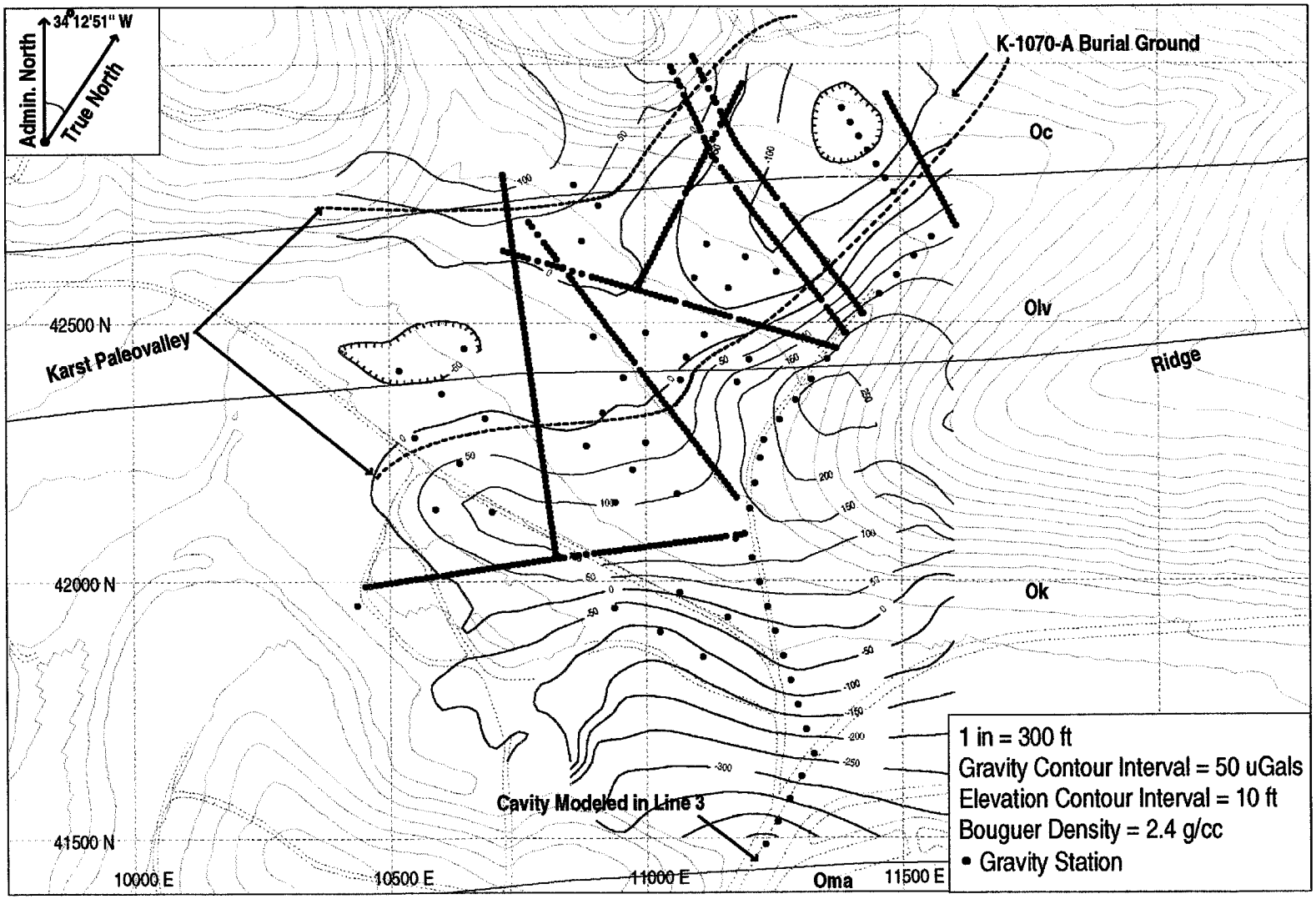


**Fig. 3-13. Contour map of the complete Bouguer gravity for the K-901 Site with the regional gradient and K-901 data subset average removed. Negative values are shown in red, and positive values are shown in blue.**

# 4. MODELING AND INTERPRETATION

Forward modeling of gravity data is a method in which the theoretical gravity response from a model of the subsurface is fit to the observed data. This method is a useful technique for the interpretation of gravity data along profile lines. An interactive two-and-one-half dimensional forward modeling program (Saltus and Blakely 1993) was used to model the observed gravity along the eleven profile lines in the study area.

Because of the inherent nonuniqueness of gravity modeling (many different models can produce the same gravity anomaly), geologic constraints and reasonable assumptions must be applied to the gravity models. Reasonable relative densities and dimensions for the underlying bedrock geology, regolith, and karst must be assigned to properly model the observed data. Information such as bedrock depths obtained from boreholes help to constrain the models in this study; however, certain parameters such as the depth to the modeled cavities are based on reasonable, but arbitrary, assumptions. The constraints and assumptions applied to the models in this study are discussed below:

## 4.1 BEDROCK GEOLOGY

Stratigraphy and geologic structure information is available from the geologic map of the K-25 area (Lemiszki 1994). The K-25 Site includes clastic rocks of the Rome Formation and carbonate rocks of the Knox Group and Chickamauga Supergroup. These rocks are faulted and folded by structures that include the Whiteoak Mountain Fault, the K-25 Fault, a syncline, and an anticline, and typically dip 45°S. The contrasting bedrock densities produce gravity anomalies that are evident as long-wavelength features on both the contour map and individual profile lines that strike across different bedrock lithologies.

Since the density *contrast* is modeled, an absolute density was assigned to the Chickamauga bedrock, and relative values for the Rome and Knox bedrock were obtained by fitting the modeled response to the long-wavelength anomalies. Watkins (1964) reported average densities of fresh Rome Formation, Chickamauga, and Knox bedrock as being 2.71 g/cc, 2.72 g/cc, and 2.78 g/cc respectively. Density measurements of fresh Maynardville Limestone located within the Oak Ridge Reservation, but outside the K-25 study area, range from 2.6 g/cc to 2.8 g/cc (Bailey and Withington 1988). Based on these measurements and accounting for some weathering, the Chickamauga bedrock was assigned an absolute density value of 2.65 g/cc. Modeled densities that best fit the observed gravity are 2.65 g/cc for the Knox Group, 2.45 g/cc for the Rome Formation, and 2.55 g/cc for a large portion of the Chickamauga limestone north of the syncline axis.

## 4.2 REGOLITH

The unconsolidated material above the bedrock surface includes a combination of saprolite, soil, and fill. The thickness of this regolith was obtained from boreholes scattered across the K-25 area (Fig. 4-1). The thickness of the regolith varies from 0 to over 70 ft and will produce significant gravity anomalies. Therefore, a regolith layer is included in the models of the gravity profile lines. The mapped bedrock elevation constrains all of the profile lines except for line 1, which lies outside the mapped area.

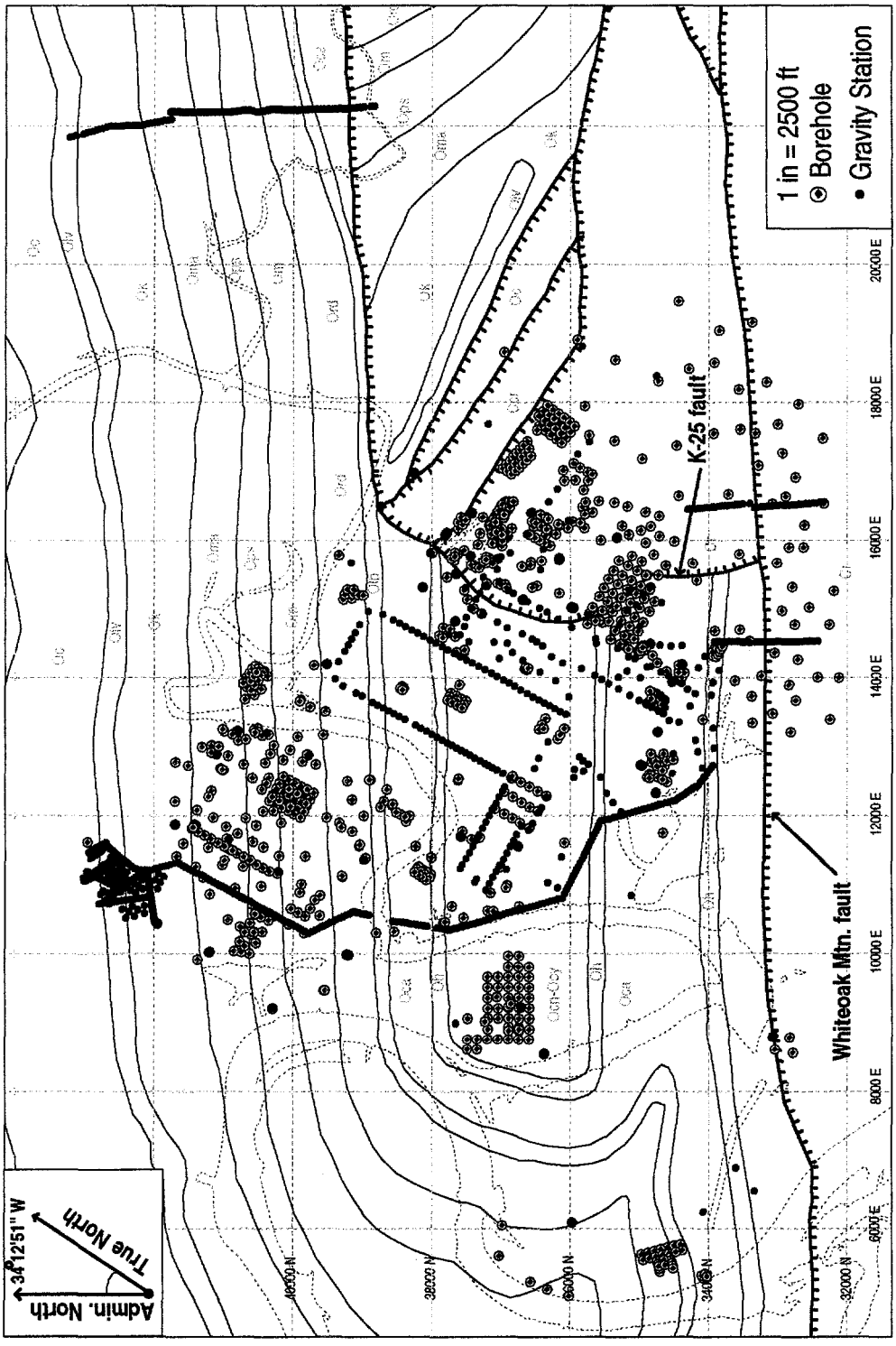


**Fig. 4-1. Locations of boreholes within the K-25 Site.**

Seventy-five bulk density measurements within K-25 show an average regolith wet density of 1.95 ±0.12 g/cc, and an average regolith dry density of 1.55 ±0.19 g/cc. Although there are saturation and compositional differences within the study area, an average moist density value of 1.9 g/cc was assigned to the regolith layer in the modeling. The effects of cut-and-fill operations may act to vary the regolith density, therefore the 1942 and current surface elevations (Coleman et al., in preparation) are included on the models to show any possible relation to the observed gravity.

## 4.3 KARST

Near-surface cavities will typically produce a short-wavelength gravity anomaly with a magnitude that is dependent upon the size and depth of the cavity and its relative density contrast with the surrounding rock. Cavities filled with water, mud, and clay have been intersected by wells in the Chickamauga and Knox carbonate bedrock at K-25 (Geraghty & Miller 1989). The observed cavities within the Chickamauga limestone have an average thickness of 4 ft, with the largest being 13 ft. Larger cavities up to 17.5 ft thick have been observed within the Knox dolomite (B. Murray [SAIC], personal communication 1995). The Knox dolomite is known to contain several large, open caves in other portions of the Oak Ridge Reservation, while no caves have been located to date within the Chickamauga limestone (Lemiszki et al. 1995).

In the gravity modeling, karst features are modeled as mud-filled cavities surrounded by bedrock. In reality, these features may be diffuse zones made up of many small cavities and weathered bedrock. Mud densities measured from a known cavity within the Maynardville Limestone ranged from 1.25-1.6 g/cc (Shevenell 1994). The modeled cavities were assigned a density of 1.4 g/cc, which corresponds to the measured values of the mud and represents a density between that of water (1.0 g/cc) and regolith (1.9 g/cc). The top of the cavities are modeled at an arbitrary depth of 20 ft below the bedrock surface, which allows a competent layer of rock to exist between the cavity and the regolith.

Cavities may produce anomalies that are similar in magnitude and wavelength to those produced by abrupt changes in regolith thickness. Fig. 4-2 shows similar anomalies resulting from a 35-ft change in regolith thickness and a mud-filled cavity approximately 20 ft thick. Because of this inherent ambiguity in the modeling, two models are presented for each profile line. Model 1 allows the regolith thickness to deviate from the mapped thickness, with no cavities present. In this model, all gravity anomalies due to near-surface structures may be attributed to variations in the regolith thickness. The average difference between the observed data and calculated gravity for model 1 is 6 μGals.

Model 2 constrains the regolith thickness to the mapped thickness and incorporates mud-filled cavities in the bedrock. In this model, all gravity anomalies due to near-surface structures may be attributed to the mapped variations in regolith thickness and mud-filled cavities. Because of the additional constraint, the calculated gravity from model 2 fits the data slightly worse than model 1, with an average difference of 23 μGals. These models are intended to represent end members of the range of possible solutions that match the data. For each profile line, the most likely cause of the anomalies will be discussed.

## 4.4 LINE 1

Line 1 (Fig. 4-3) lies outside of the area constrained by the bedrock elevation map and the 1942 surface elevation map. Many bedrock outcrops exist along the southern half of line 1, indicating a thin

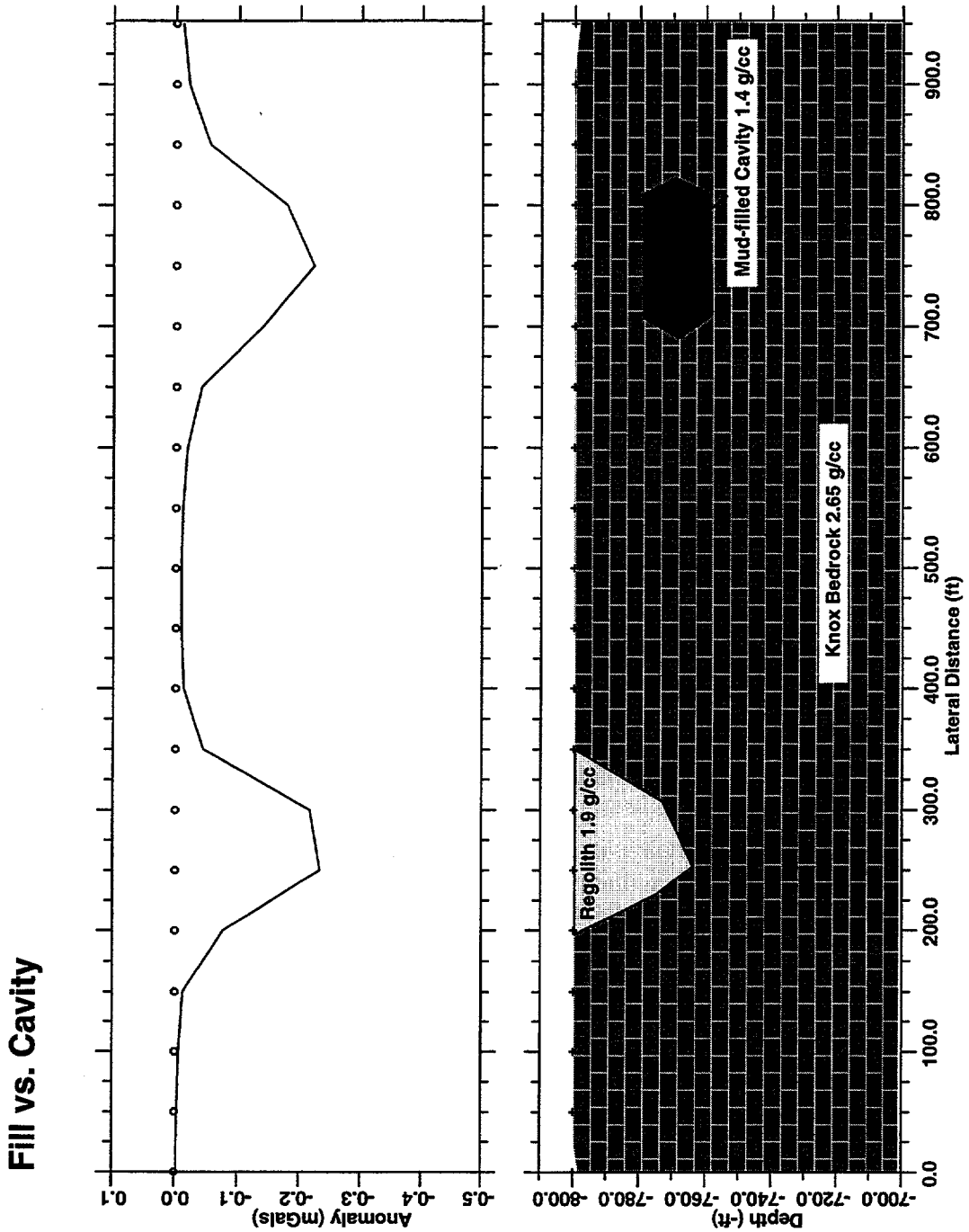


**Fig. 4-2. Model showing similar gravity anomalies resulting from a mud-filled cavity and increasing fill thickness.**

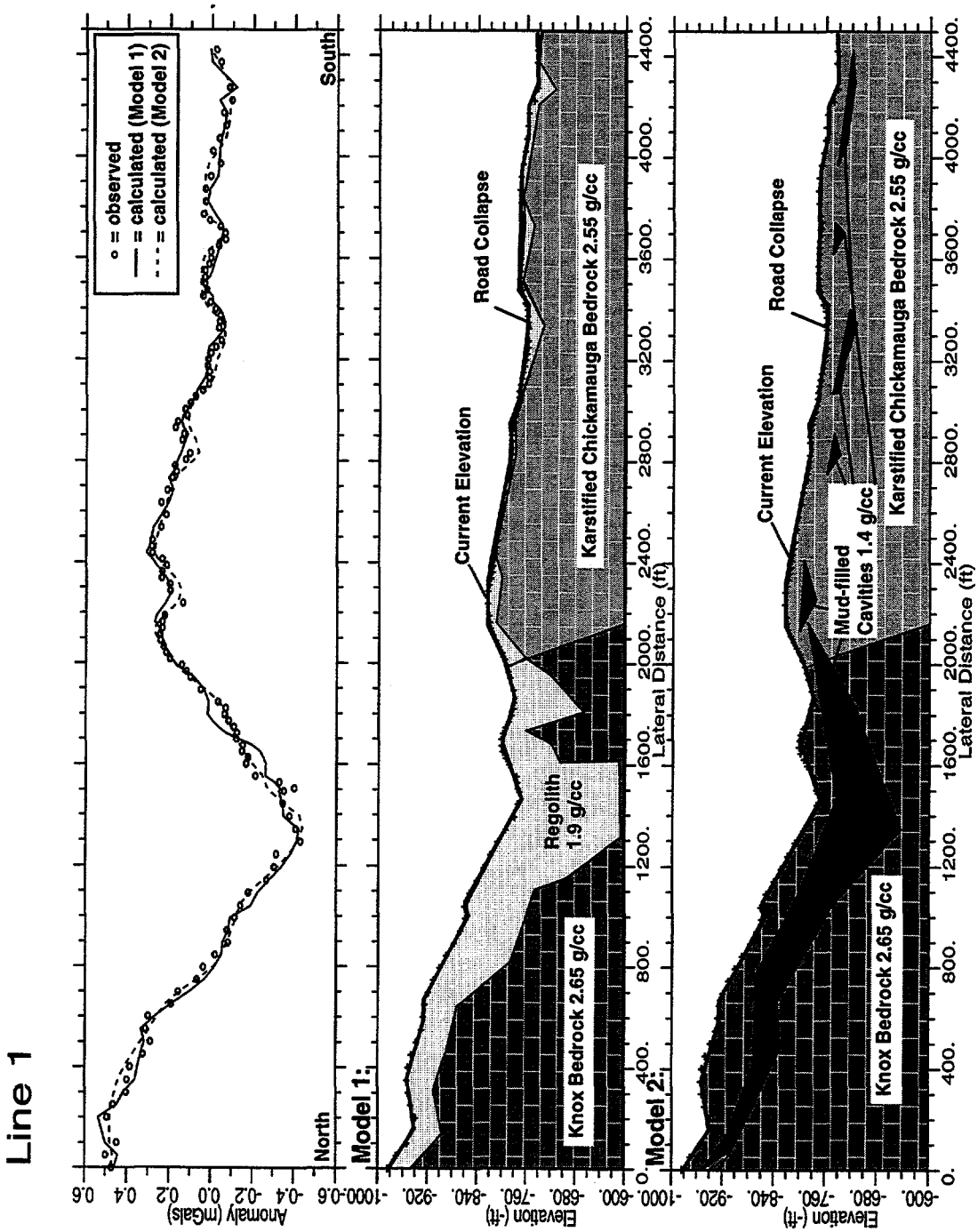


Fig. 4-3. Models of profile line 1.

regolith layer. In model 1, the regolith thickness is set to 0 near areas of bedrock outcrops, and negative gravity anomalies are modeled as increased regolith thickness. Model 2 assumes a constant regolith thickness, and all near-surface gravity anomalies are attributed to mud-filled cavities. The line is dominated by a large 700-μGal gravity low centered 1300 ft from the north end of the line in the Mascot Dolomite (Oma) and 200 ft north of East Fork Road. In model 1, this anomaly is modeled as large increase in the regolith layer that is over 170 ft thick between 1300-1600 ft. Model 2 shows a mud-filled cavity up to 110 ft thick at this location. Clearly, the large regolith layer in model 1 and the single large cavity in model 2 do not represent realistic subsurface features. The anomaly may be best interpreted as the result of many smaller cavities concentrated in the Mascot Dolomite (Oma) near 1300 ft. This intense karstification may play a significant role in the flow of groundwater through this area.

There are several smaller anomalies (100-200 μGals) along the southern portion of line 1 that are modeled as small variations in regolith thickness in model 1 and as cavities less than 20 ft thick in model 2. One of these anomalies, centered at 3200-3400 ft, is modeled in more detail in Fig. 4-4. In December 1995, after the data had been acquired along line 1, a collapse feature was discovered along the line, 3330 ft from the north end. The collapse occurred within the dirt road and is shown in a photograph in Fig. 4-5. In January 1996, the collapse was approximately 3 ft deep, 3 ft in diameter, and filled with soil and pieces of limestone bedrock. It appeared to be expanding to the north. The collapse may be a doline associated with a 10-20 ft thick, mud-filled cavity shown in model 2. Nearby rock outcrops make the increased regolith thickness of model 1 unlikely. A larger doline, 150 ft west of the collapse, supports model 2 and may be related to the same modeled cavity.

### 4.5 LINE 2

Line 2 (Fig. 4-6) shows a strong decrease in gravity to the south corresponding to the southward thickening Rome (Cr) thrust sheet. The fault separating the Chickamauga bedrock from the overthrust Rome bedrock is modeled to dip to the south at an angle of 28°. Model 1 shows a deviation from the mapped regolith thickness of up to 50 ft near the center of the line. Since the depth to bedrock along line 2 is constrained by five nearby boreholes, a 50-ft change in regolith thickness is unlikely.

Model 2 presents an alternative explanation with a mud-filled cavity ranging from 10-30 ft in thickness, centered at 1000 ft. This cavity may be part of an interbedded, karstified carbonate layer within the Rome thrust sheet. The anomaly is similar and in approximately the same north-south position as a modeled cavity along line 10 to the west, indicating an east-to-west lateral continuity. Deviations from the mapped regolith thickness of 10-20 ft may be valid explanations for the observed gravity at the north and south ends of the line.

### 4.6 LINE 3

The most striking anomaly present on line 3 (Fig. 4-7) is a 700 μGal gravity low centered 1200 ft from the north end of the line. The anomaly is located within the Kingsport (Ok) and Mascot (Oma) formations and has the same magnitude as the large low in line 1. Model 1 describes the anomaly as a large change in the regolith thickness that is 140 ft thick at its center. Nearby wells and boreholes show the depth to bedrock to be 0-20 ft thick in this area, making the modeled regolith thickness an unlikely interpretation for the anomaly. Model 2 describes the anomaly as a series of mud-filled cavities up to 70 ft thick. As in line 1, the modeled cavity is more realistically described as a concentration of smaller cavities and may represent intensely karstified dolomite.

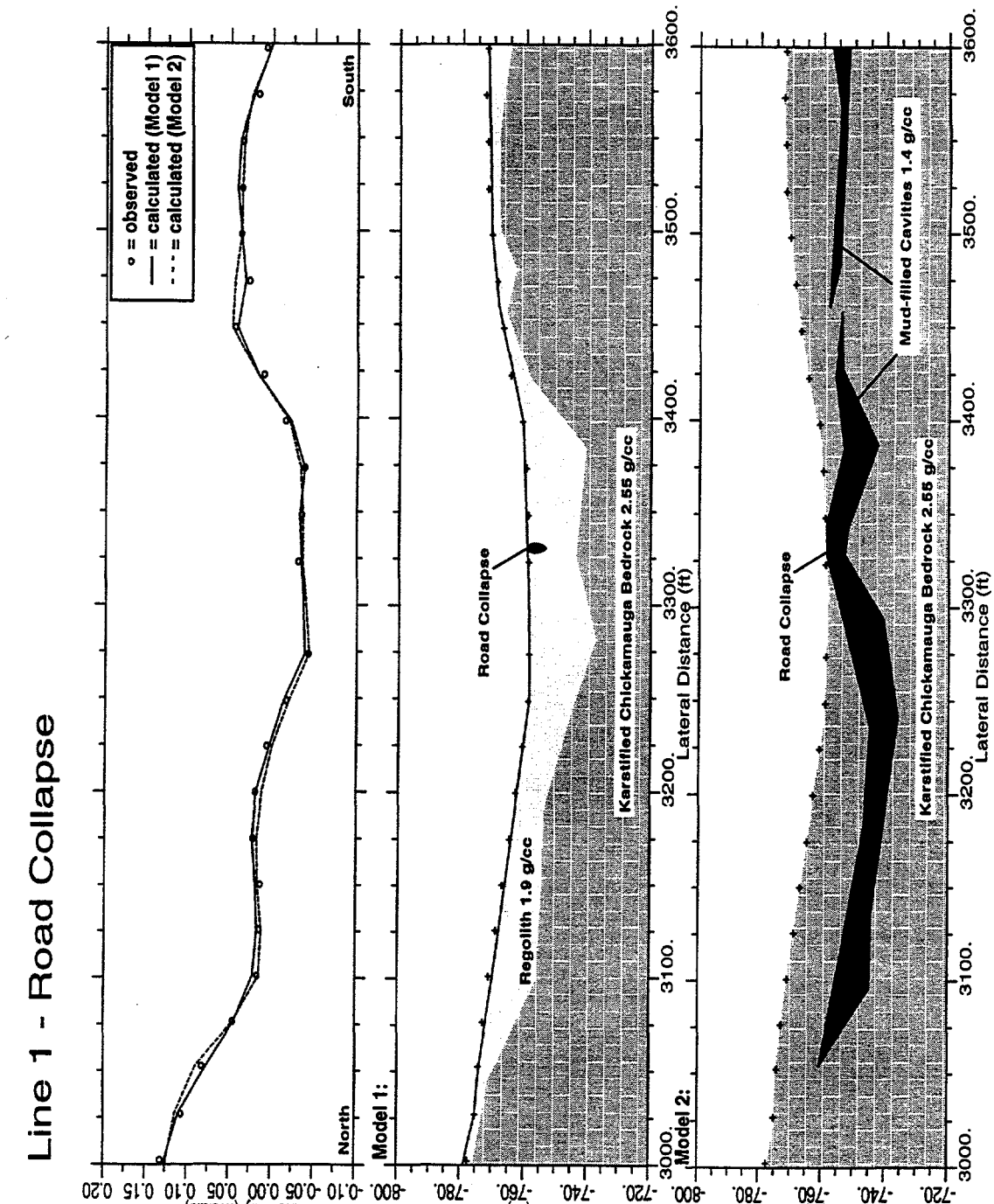


**Fig 4-4. Detailed models of line 1 near the road collapse.**

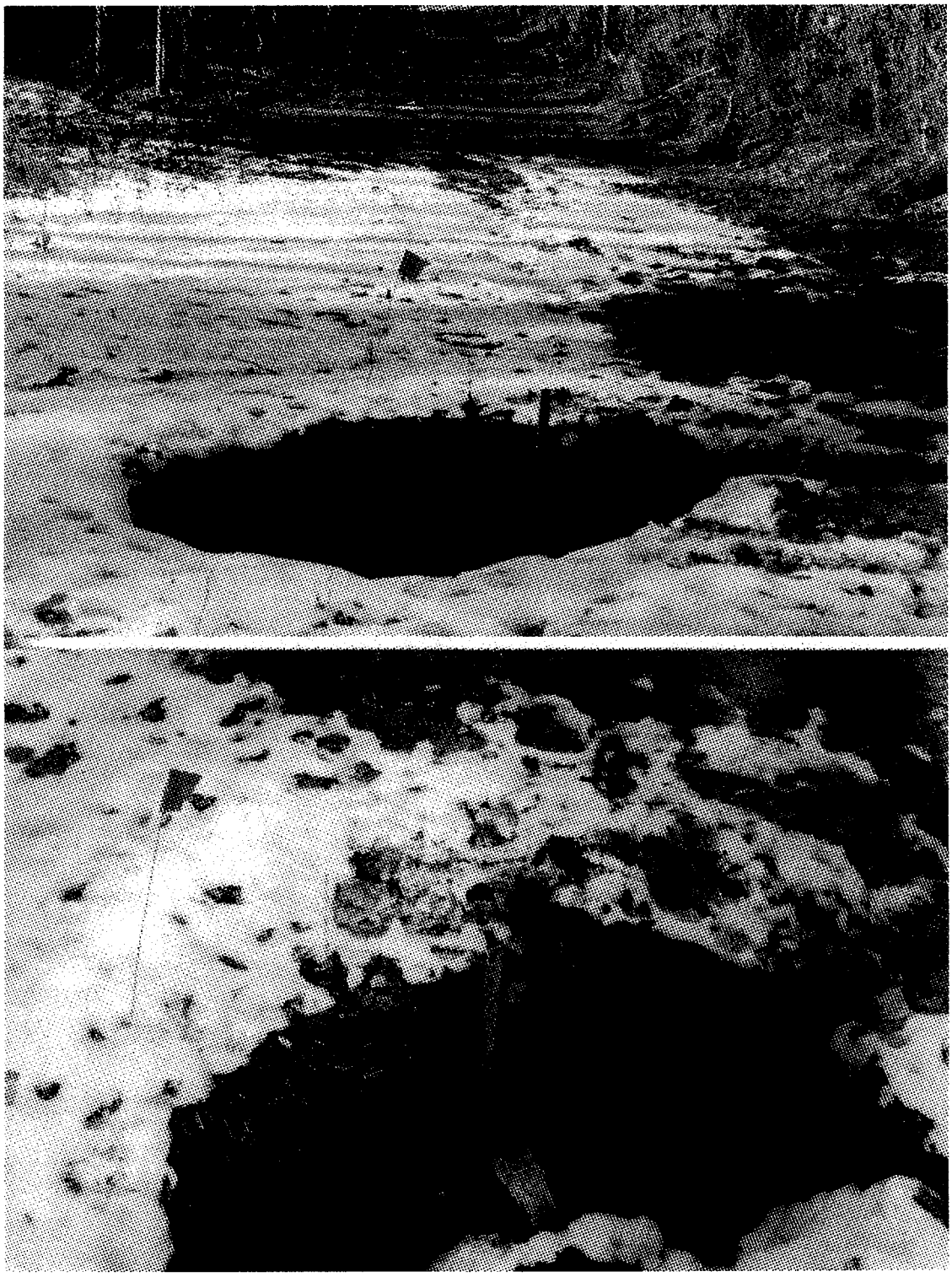

**Fig. 4-5. Photographs of the road collapse along line 1.**

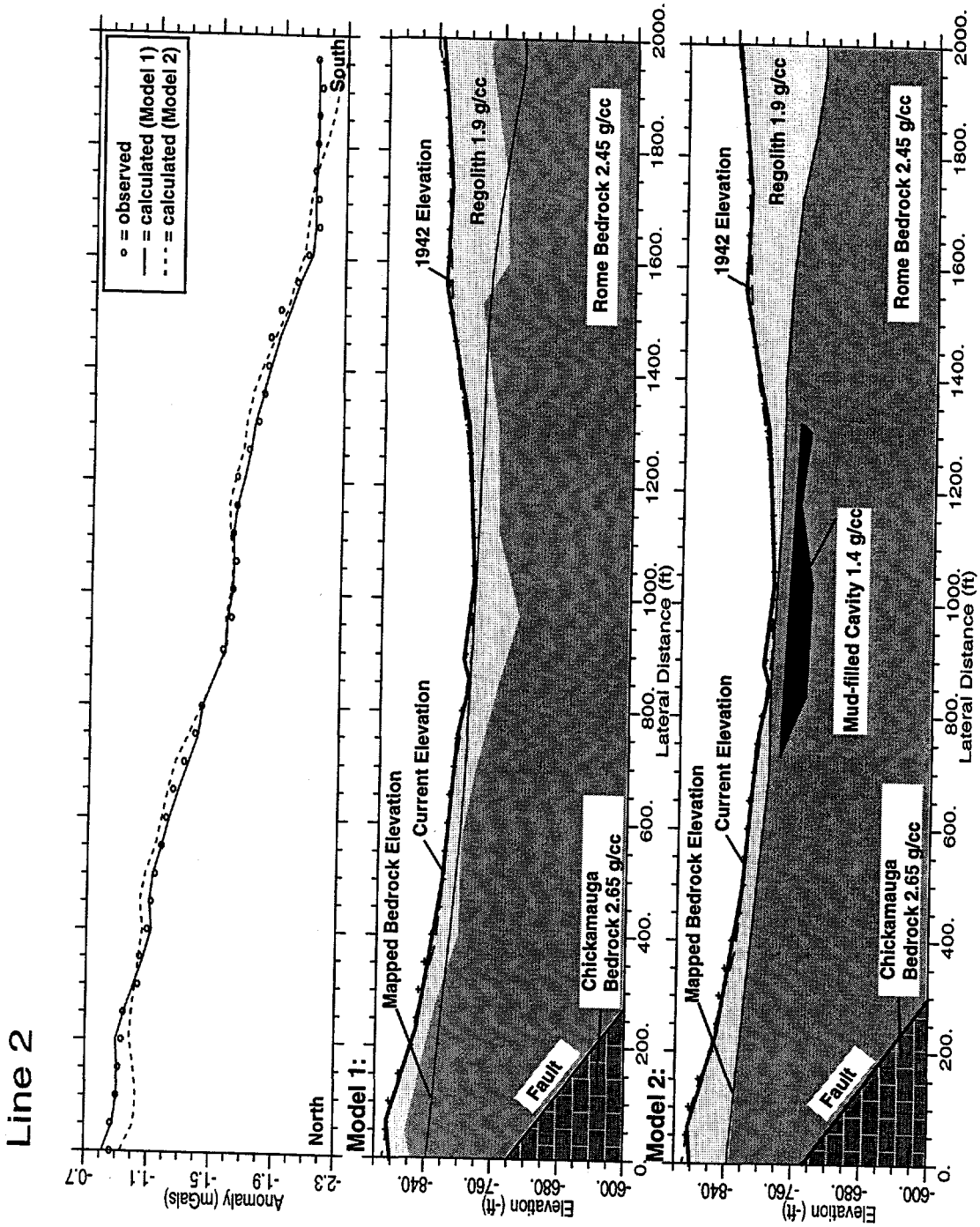


**Fig. 4-6. Models of profile line 2.**

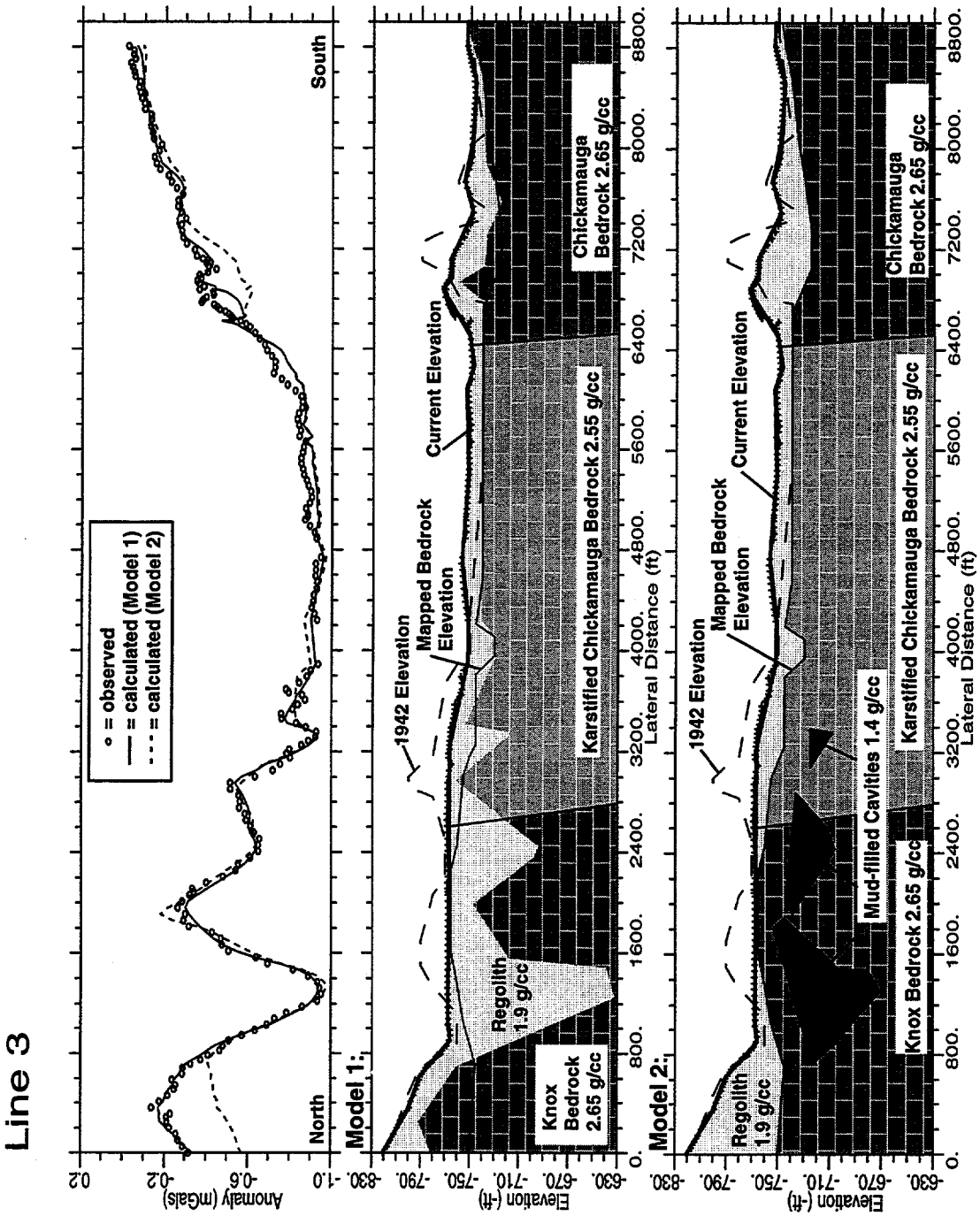


**Fig. 4-7. Models of profile line 3.**

It is interesting to note that the two large gravity lows present in lines 1 and 3 occur within the same geologic formation. Fig. 4-8 shows gravity profiles from portions of lines 1 and 3 that pass through the same formations. The lateral positions along line 1 have been warped to fit the boundaries of the formation contacts crossed in line 3 so that a comparison of the two profiles may be made. The large anomalies along both lines have similar magnitudes and wavelengths, possibly indicating a similar subsurface structure. The anomaly in line 3 is shifted approximately 300 ft north of the line 1 anomaly. The location of the anomalies supports a model containing a laterally continuous zone of karstification within the Kingsport (Ok) and Mascot (Oma) formations; however, more gravity stations between the two lines are necessary to define the spatial continuity of the gravity lows.

Line 3 shows the gravity contrast within the Chickamauga that is consistently observed in all profile lines that cross the syncline axis. Fig. 4-8 shows that the gravity values within the Chickamauga north of the syncline axis along line 3 average 350 μGals lower than the values from the same formations along line 1. Also, the gravity values observed within the Carters Limestone (Oca) lying north of the syncline axis average 750 μGals lower than the values within the Carters Limestone (Oca) south of the axis.

There is no correlation between the observed gravity contrast in the Chickamauga and mapped regolith thickness, so the contrast is assumed to be due to bedrock density differences within the Chickamauga. North of the syncline axis, the Chickamauga bedrock has a modeled density of 2.55 g/cc, while south of the syncline axis, the Chickamauga bedrock has a modeled density of 2.65 g/cc. The density contrast is unusual since the same formations (Oca, Ocn-Ocy, Oh) are exposed symmetrically about the syncline axis. The north side of the low is not constrained by the syncline, and no evidence for denser bedrock is seen until the Knox dolomite is reached to the north. Since the bedrock lithology does not change across the syncline axis, the modeled density contrast may be attributed to increased karstification within the Chickamauga, north of the syncline axis. A 7.1% increase in mud-filled cavities (modeled with a density of 1.4 g/cc) within the northern portion of the Chickamauga would explain the contrasting Chickamauga density.

### 4.7 LINE 4

The majority of line 4 (Fig. 4-9) lies within the Chickamauga north of the syncline axis. Model 1 shows regolith deviations of up to 40 ft from the mapped thickness to match observed anomalies of approximately 200 μGals. The mapped regolith thickness is only constrained by boreholes at the north end, south end, and 1000-1500 ft from the north end of the line. At these positions, the calculated gravity from the mapped regolith thickness fits the observed data, and anomalies in other portions of the line may in fact be due to regolith variability. Alternatively, Model 2 describes the anomalies as mud-filled cavities up to 30 ft thick. The 1942 elevation compared with the current elevation shows that the southern portion of the line has had up to 30 ft of regolith cut and removed, which may increase the variability in the observed gravity. The line crosses the syncline axis at 2700 ft, where the less karstified Chickamauga bedrock south of the axis fits the data.

### 4.8 LINE 5

A 500 μGal gravity low is evident at the southern portion of line 5 (Fig. 4-10), and is also evident in lines 7 and 8. The mapped regolith thickness increases to 60 ft at the southern end of the line. Model 1 shows that a regolith thickness of up to 90 ft fits the observed gravity low, while model 2 shows that a 20-ft-thick, mud-filled cavity may also explain the gravity low. Since the gravity low occurs at the

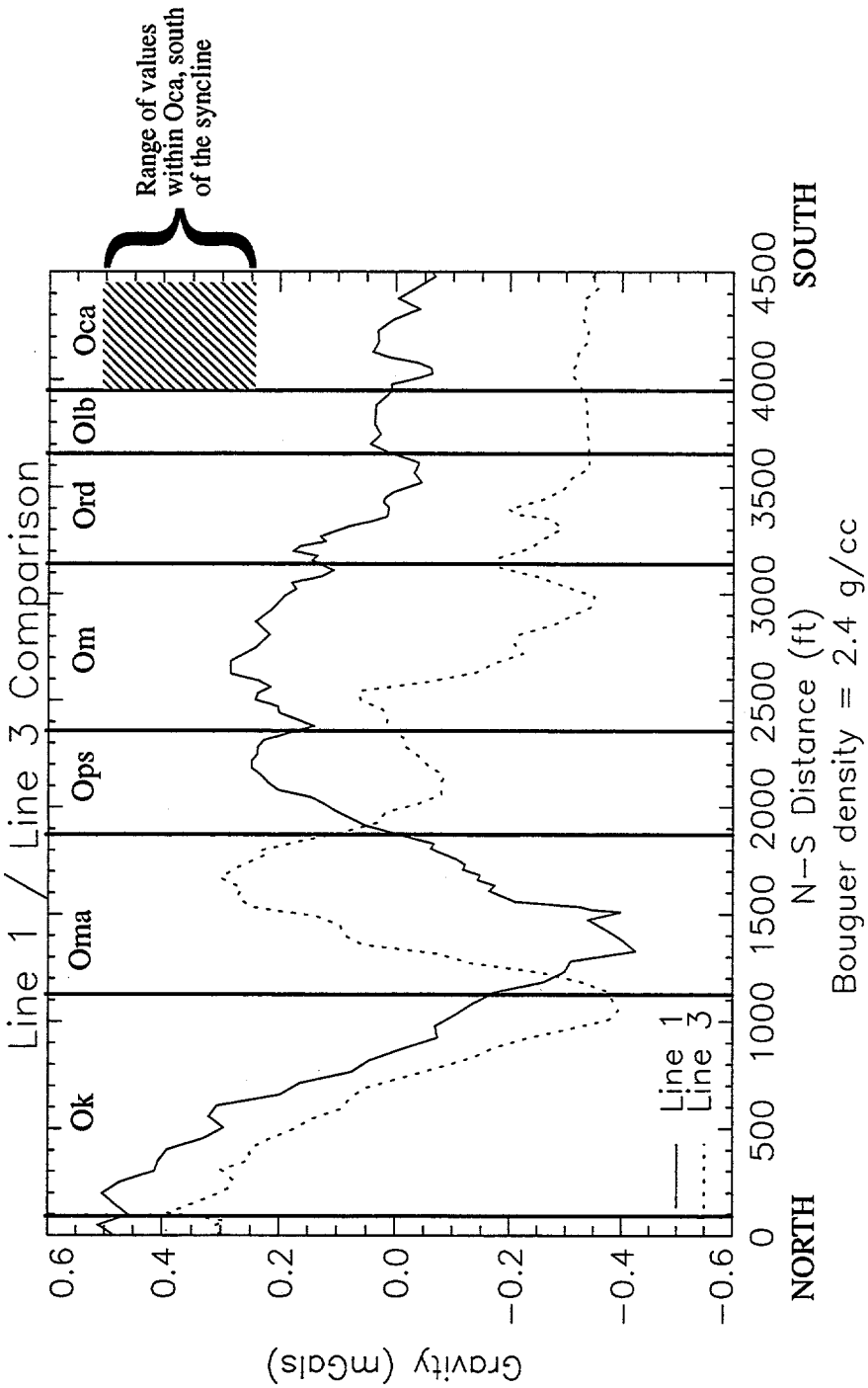


**Fig. 4-8. Comparison of lines 1 and 3 through the same geologic formations.**

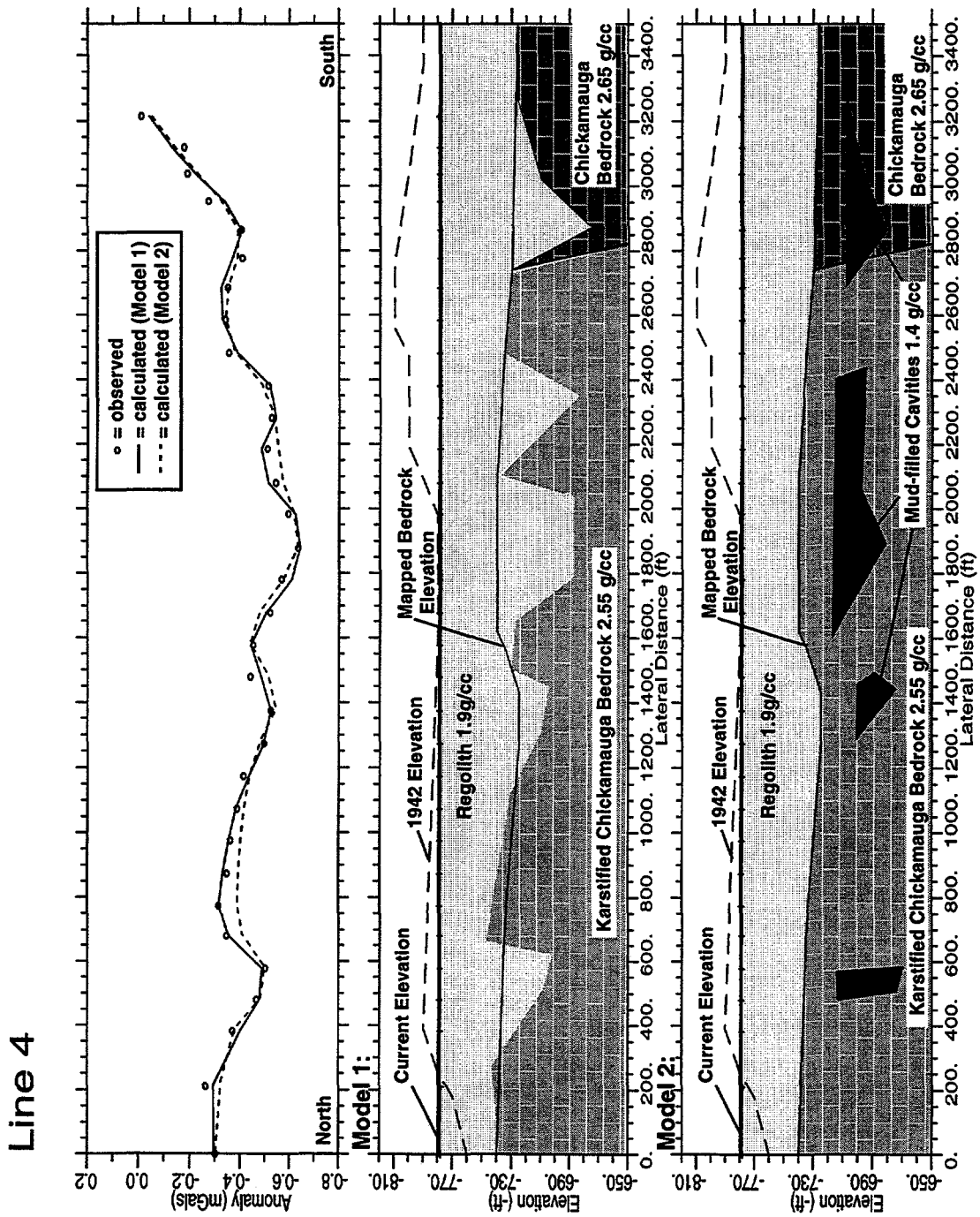


**Fig. 4-9. Models of profile line 4.**

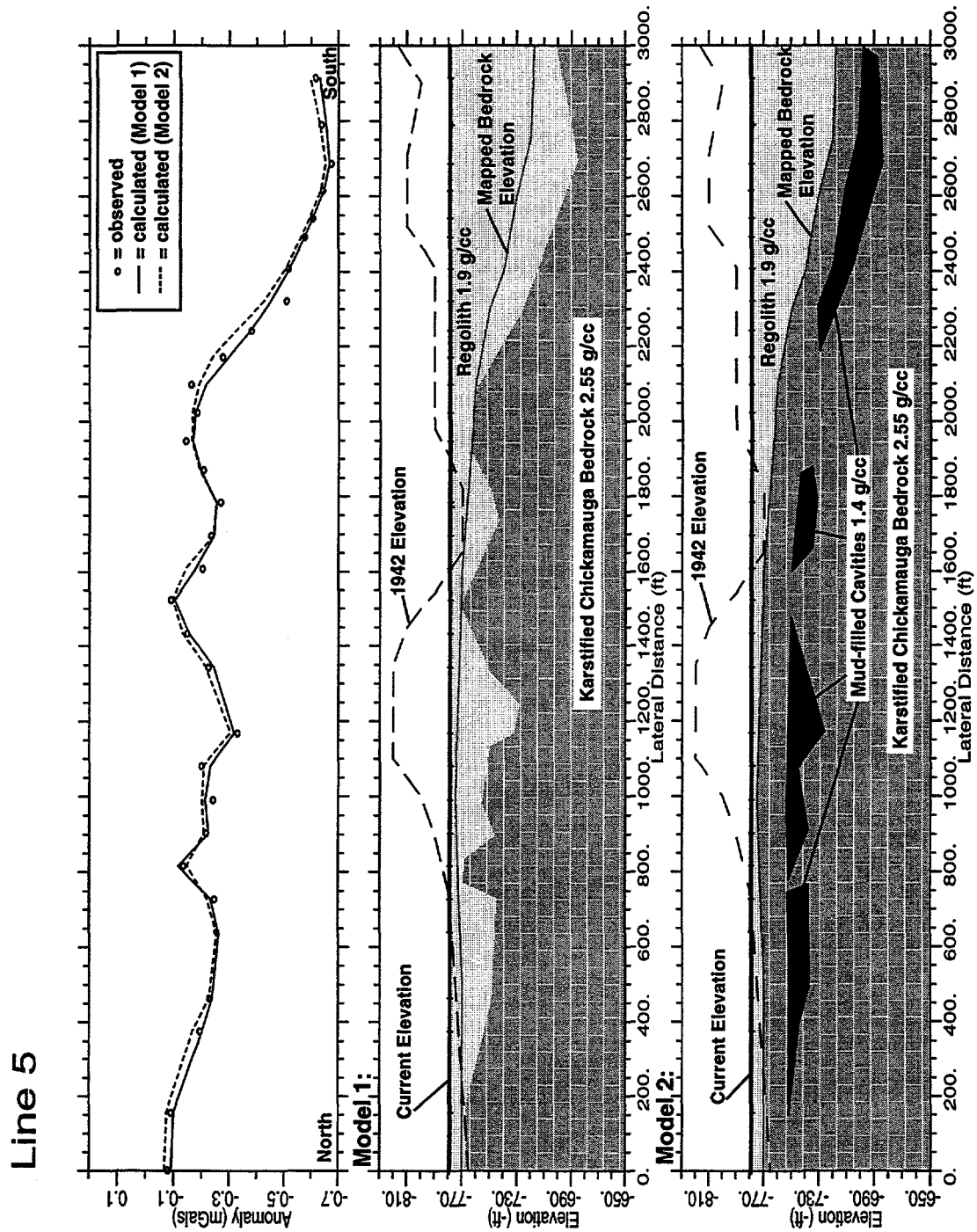


**Fig. 4-10. Models of profile line 5.**

mapped location of increased regolith thickness, model 1 is the most realistic of the two models. The majority of the line is not well constrained by boreholes, and deviations from the mapped regolith thickness can be expected. Variations in the regolith thickness of 5-40 ft are modeled along the northern and middle portions of the line.

### 4.9 LINE 6

Line 6 (Fig. 4-11) runs east from the K-25 building, and crosses the mapped K-25 fault 500 ft from the west end of the line. Although this fault is currently thought to separate the thin Rome thrust sheet to the east from the Chickamauga to the west, no evidence for the fault is apparent in the data along line 6. It is possible that the fault exists, but separates bedrock of roughly the same density. Well logs east of the fault at this location show a thin (~20 ft) layer of shale over limestone, and, in some cases, a gradual transition from shale to the underlying limestone (Geraghty & Miller 1989). The shale may be part of the Conasauga Group, although it is not currently mapped at this location. The gravity models assume that there is no density contrast between the Chickamauga bedrock west of the fault, and the combination shale/limestone bedrock lithology east of the fault.

The regolith layer along line 6 is constrained by boreholes along its entire length. Model 1 shows deviations of the regolith thickness of up to 40 ft from the mapped thickness to match the observed gravity anomalies. The anomaly located 2350 ft from the west end of the line is only constrained by one gravity measurement, so the validity of that anomaly is questionable. Model 2 shows mud-filled cavities of up to 35 ft thick to explain the variations observed in the gravity. Since the regolith thickness is constrained along the entire length of the line, the gravity anomalies may be due to concentrations of small cavities at the locations shown in model 2. It is possible that the cavities lie in the limestone bedrock beneath the shale layer.

### 4.10 LINE 7

Line 7 (Fig. 4-12) starts at the west end of the K-27 building and crosses the syncline axis at an oblique angle to the east. This line shows further evidence that the syncline axis separates less karstified Chickamauga rock to the south from the Chickamauga to the north. The large gravity low at the west end of the line is part of the same anomaly crossed by line 5 and is due to increased regolith thickness. The modeled regolith thickness in model 1 fits the mapped thickness reasonably well along this line and has a maximum thickness of 65 ft centered around the gravity low. The west and east ends of model 1 require a thinner regolith layer than that currently mapped. A large deviation centered at 3100 ft is due to a gravity anomaly constrained by only one observation, so the validity of that anomaly is questionable. A 200-μGal anomaly centered at 4000 ft is modeled as a 25 ft deviation from the mapped regolith thickness in model 1 and a 15 ft mud-filled cavity in model 2. A similar size cavity is modeled at 1000 ft in model 2.

### 4.11 LINE 8

Line 8 (Fig. 4-13) parallels the southern side of the K-27 building and lies north of the syncline axis. The regolith thickness is constrained by boreholes on the west and east ends of the line. The observed gravity becomes gradually lower from west to east due to the thickening regolith. The thickest portion of the mapped regolith is 65 ft and is part of the same thick area observed in lines 5 and 7. The gradual trend is interrupted near the center of the line by a steeper gravity low that is modeled as a 55-

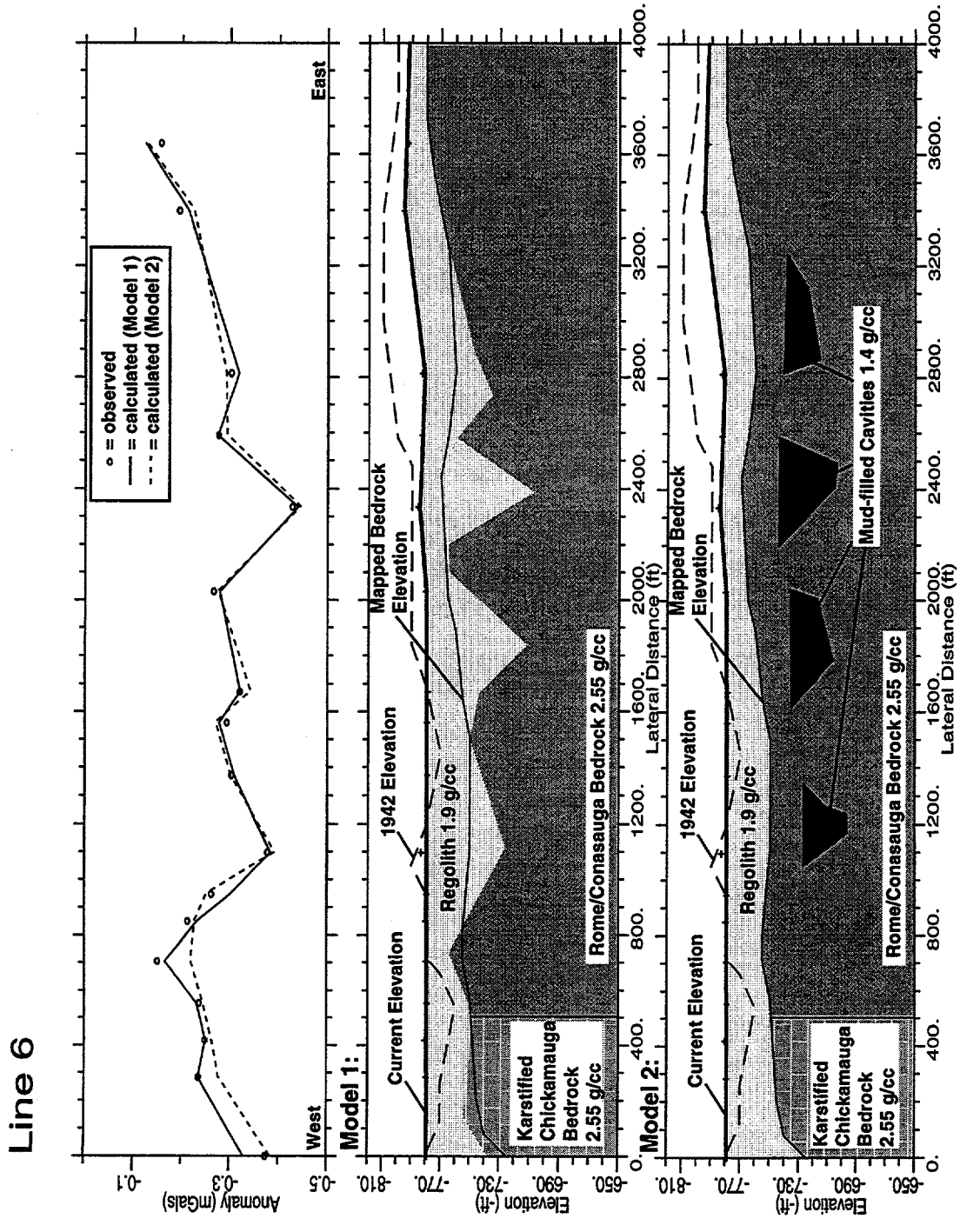


**Fig. 4-11. Models of profile line 6.**

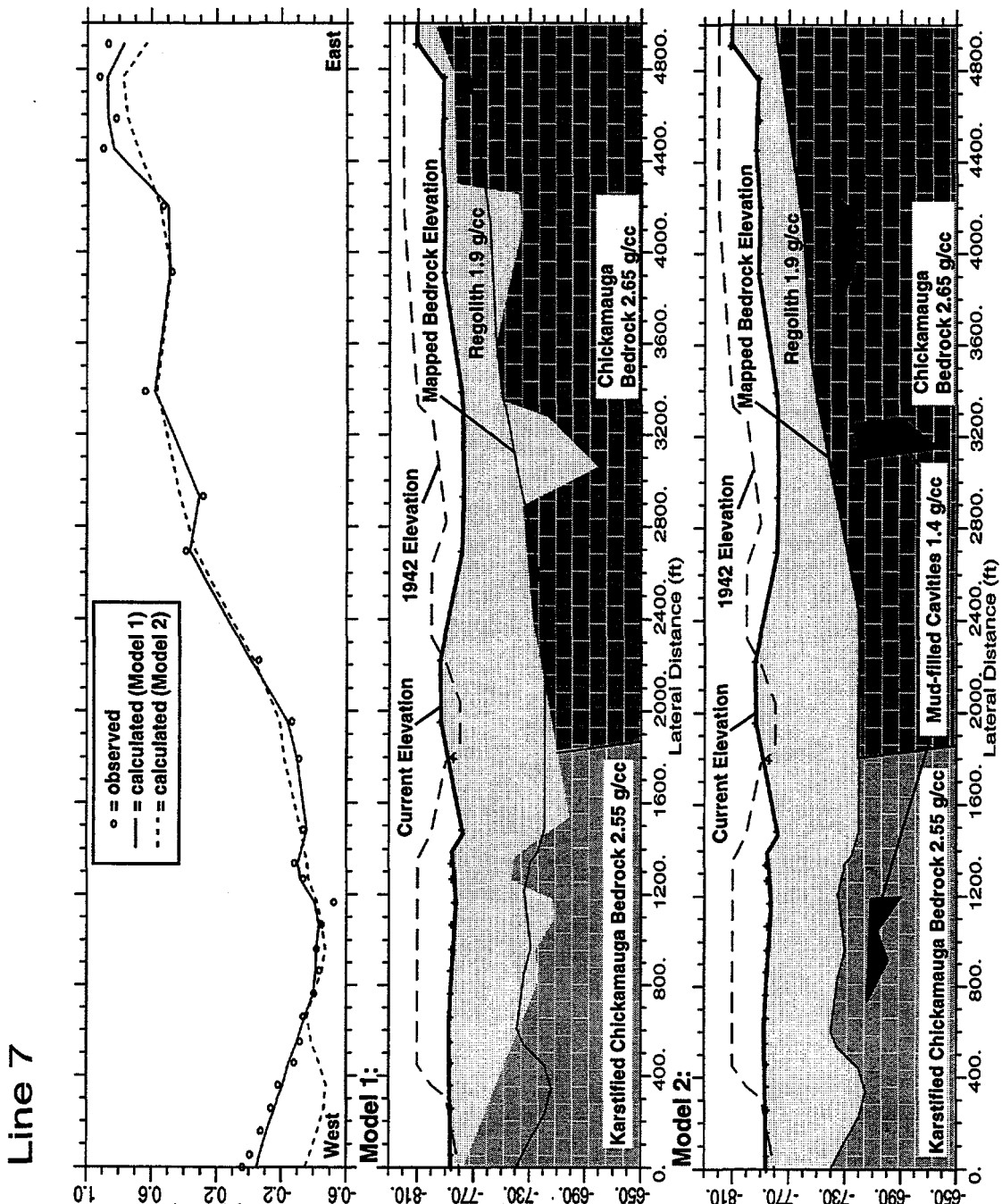


**Fig. 4-12. Models of profile line 7.**

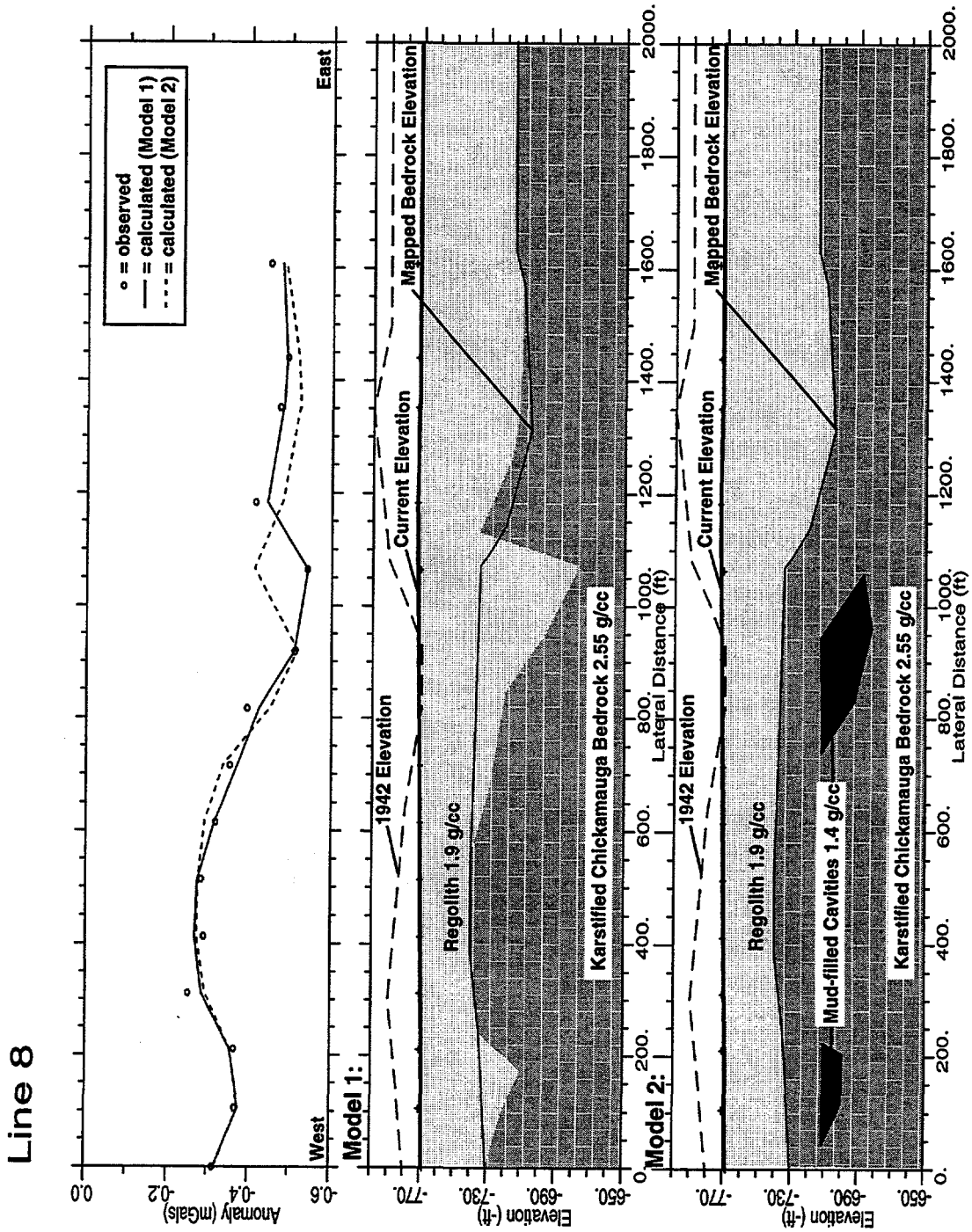


**Fig. 4-13. Models of profile line 8.**

ft deviation from the mapped regolith thickness in model 1 and a 20- to 30-ft thick, mud-filled cavity in model 2. At the west end of the line, there is a 10-20 ft deviation in the mapped regolith thickness in model 1 and a 10 ft mud-filled cavity in model 2, which represents the observed 100- μGal anomaly at this portion of the line.

### 4.12 LINE 9

Line 9 (Fig. 4-14) starts at the northwest corner of the K-1401 building and parallels line 11. The profile shows evidence for the K-25 fault at approximately 1700 ft, where a 500-μGal increase in gravity indicates the transition from the overthrust shales and underlying karstified limestone to less karstified Chickamauga limestone. The modeled fault is approximately 500 ft south of its currently mapped position.

Model 1 shows that a majority of the modeled regolith thickness along the line is in good agreement with the mapped thickness. There is a 10-20 ft deviation from the mapped thickness between 2300 ft and the south end of the line. Model 2 shows this area as having an irregularly shaped, mud-filled cavity of up to 25 ft thick. Two sharper deviations centered at 1400 ft and 2900 ft are based on gravity anomalies constrained by one observation each and may not be valid.

### 4.13 LINE 10

Line 10 (Fig. 4-15) shows a clear indication of the Whiteoak Mountain Fault starting approximately at 1000 ft. The gravity drops 700 μGals in a lateral distance of only 500 ft. The surface location of the fault is modeled approximately 400 ft south of its currently mapped position. The fault is modeled with a dip of 45° to the south, and divides the Chickamauga bedrock from the overthrust Rome (Cr) bedrock.

Model 1 shows a broad, thick regolith layer between 200-900 ft, that deviates up to 30 ft from the mapped thickness. Since line 10 is constrained by boreholes that show shallow depths to bedrock at this location, this broad, thick regolith layer is unlikely. Model 2 shows a 10-25 ft thick mud-filled cavity at this same location. The cavity is in the same north-south position as the one modeled in line 2, possibly indicating a continuous east-west zone of karstification between these two lines.

### 4.14 LINE 11

Line 11 (Fig. 4-16) starts at the northeast corner of the K-1401 building and parallels line 9. A 450-μGal increase in gravity beginning at 2500 ft is evidence for the K-25 fault. The fault is modeled approximately 800 ft south of its currently mapped position and divides the shale and underlying karstified limestone to the north from the less karstified Chickamauga limestone to the south.

Model 1 shows that the modeled regolith thickness does not fit the mapped thickness. There is a large 45-ft thickness deviation at the north end of the line and a 25-ft thickness deviation at the south end of the line. Since both of these regions are constrained by boreholes, the cavities shown in model 2 may be a more realistic interpretation of the gravity anomalies along this line. Model 2 shows a mud-filled cavity up to 40 ft in thickness at the north end of the line and a 20-ft-thick, mud-filled cavity between 2900-3700 ft. As in the previous models, the cavities may represent concentrations of smaller cavities and not one single large cavity.

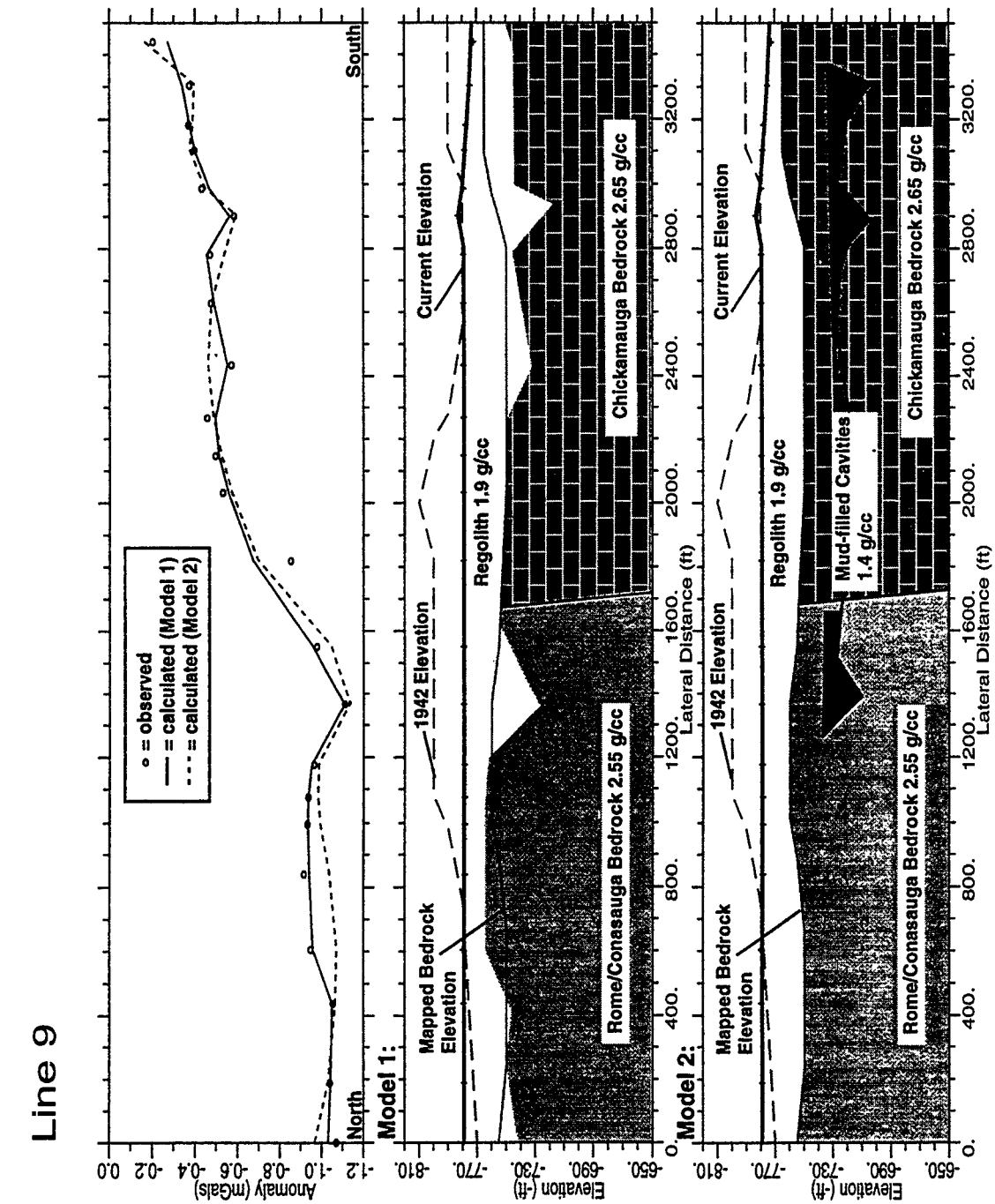


**Fig. 4-14. Models of profile line 9.**

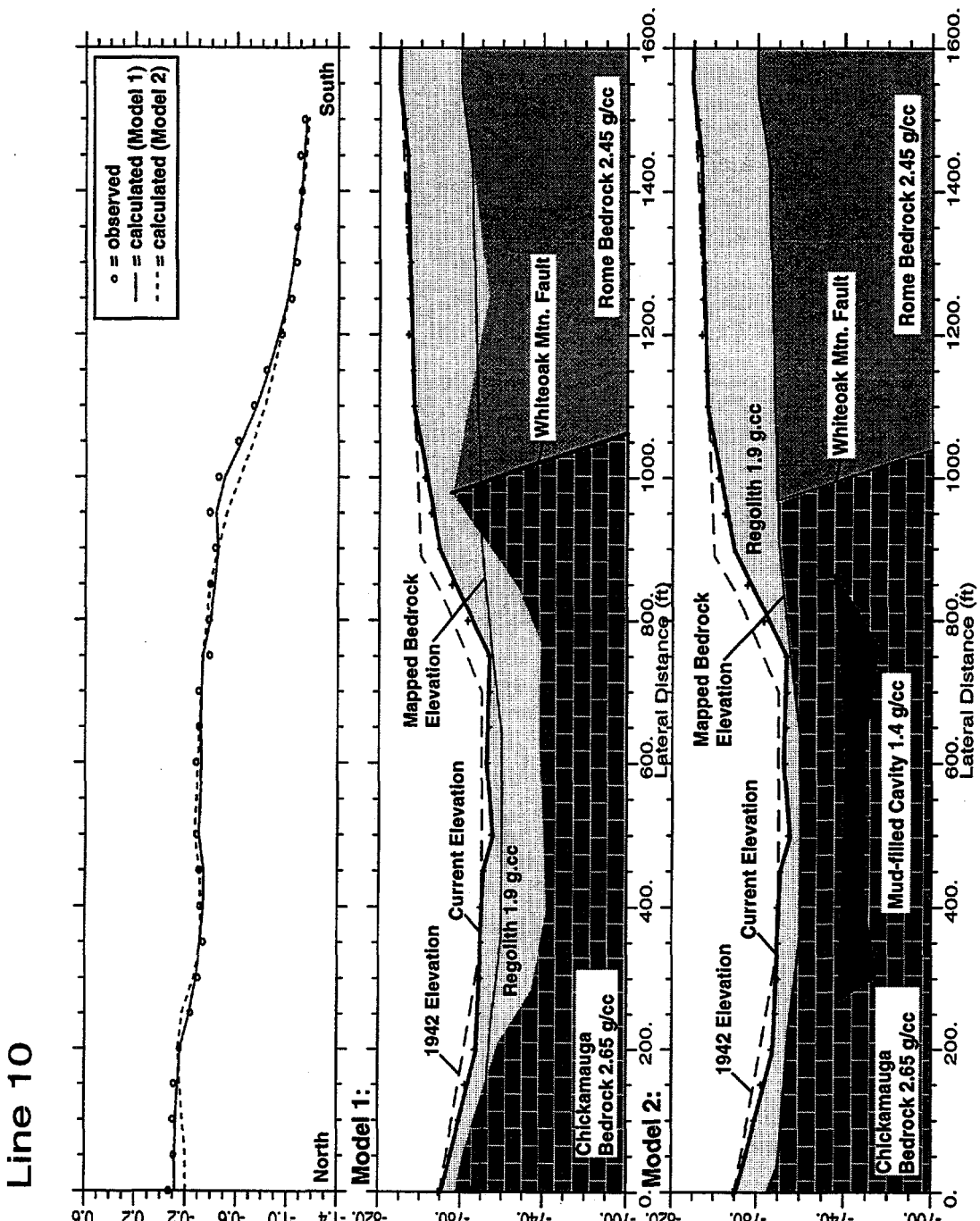


**Fig. 4-15. Models of profile line 10.**

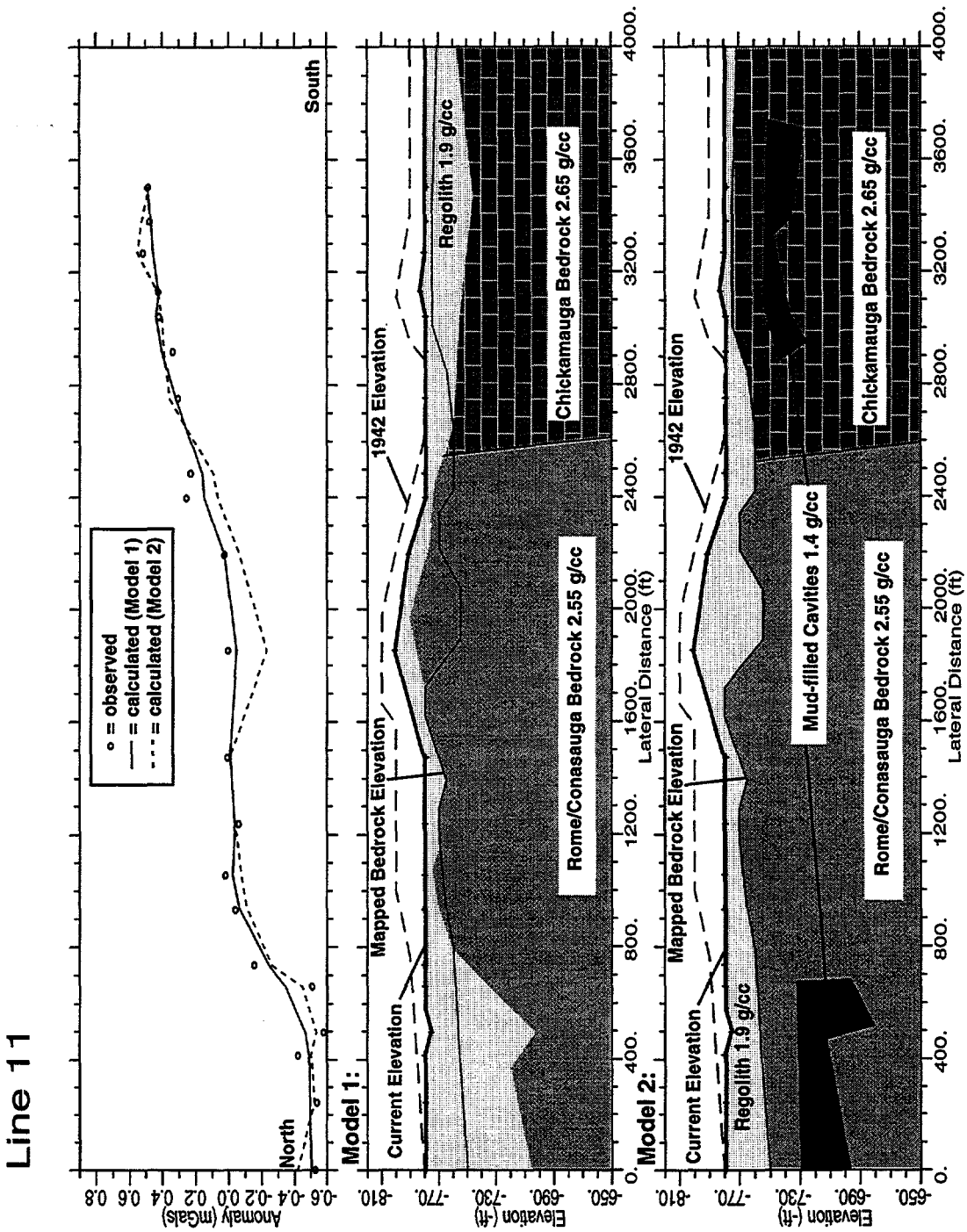


**Fig. 4-16. Models of profile line 11.**

## 4.15 K-25 GRAVITY MAP

The K-25 complete Bouguer gravity map (Fig. 3-12) shows the contoured gravity observations on a plant-wide scale annotated with the major features identified from the modeling of the profile lines. The gravity map includes all data from the profile lines and individual stations scattered throughout the study area. Faults, geologic contacts, mapped sinkholes, and stream boundaries are shown on the gravity map.

The Whiteoak Mountain fault appears as a strong, north-to-south, negative gravity gradient delineated by lines 2 and 10. This fault separates the Rome Formation in the hanging-wall from the Chickamauga Supergroup in the footwall west of the northwest-striking K-25 fault. East of the K-25 fault, geologic observations suggest that a thin slice of the Rome Formation (Cr) overlies Chickamauga carbonates north of the Whiteoak Mountain fault (Lemiszki 1994). However, within the northern portion of the mapped thin Rome thrust slice, there are low gravity values that are inconsistent with a northward thinning slice of Rome shales over denser carbonates. The gravity low in the north section of the slice seems to be striking parallel to faults bounding the thrust slice to the northeast. The low gravity values are of the same magnitude as those found within the syncline, west of the K-25 Fault. It is for this reason that no significant signature of the K-25 Fault is evident in line 6, which crosses into the northern section of the thrust slice.

Lemiszki suggests that the northern section of the mapped slice may actually be dissected by a northwest striking fault and composed of Conasauga Group shale that has a lower density relative to the Chickamauga limestone. Another possible interpretation, supported by the observed continuity of the gravity across the K-25 fault, is that the karstified Chickamauga bedrock located north of the syncline axis continues beneath the thin Rome slice to the east. A seismic reflection profile at this location shows evidence that the syncline does continue laterally beneath the Rome slice.

Most of the localized anomalies that may be due to karst or regolith thickness variations are best seen in the individual profiles. However, three of the largest anomalies due to near surface features are clearly evident in the contour plot. The 800-μGal low centered at administrative coordinates 12100E, 37100N is modeled as increasing regolith thickness. Models from lines 5, 7, and 8 show the regolith thickening up to 90 ft within the anomalous region. Nearby boreholes support the thick regolith models. The large 700-μGal lows observed along Lines 1 (22100E, 41900N) and 3 (11200E, 41400N) near the Mascot (Oma) and Kingsport (Ok) contact are evident in the contour plot, although their magnitudes have been reduced due to the averaging of the gridding routine.

Both of these anomalies are modeled as large cavities, but may realistically represent concentrated areas of smaller cavities. Such cavities may form a major east-to-west conduit for the groundwater, but more data are needed to determine the continuity of the anomaly between lines 1 and 3. It is interesting to note that these large anomalies are both located near previously identified, large sinkholes. The sinkholes may be the surface expression of the karst features responsible for the gravity anomalies. Similarly, the road collapse along line 1 may be a doline leading to a modeled mud-filled cavity.

## 4.16 K-901 GRAVITY MAP

The K-901 complete Bouguer gravity map (Fig. 3-13) shows the relative gravity highs and lows within the K-901 data subset, along with elevation contours and geologic contacts. The regional gradient in this data subset is consistent with the regional gradient in the K-25 area and was removed from the data. Because the average gravity value within the subset is removed from the data, the values are statically shifted by -85 μGals from the full data set. The map includes stations occupied in previous

studies (Wilson and Ketelle 1992; Coleman Energy & Environmental Systems 1994), a portion of line 3, and interspersed stations added as a part of this study.

The southeastern portion of the area contains a gravity gradient, decreasing from 0 to -400 μGals over a distance of 600 ft, that is associated with the 700 μGal low observed in line 3. An east-to-west striking gravity high across the central portion of the study area separates the gravity low to the south from a low in the northern portion. The southern part of the gravity high trends parallel to the base of a ridge located to the east of the study area, and the northern part trends parallel to a flank of a ravine that extends out of the study area to the northeast. The correlation with topography may represent the westward extension of relatively shallow bedrock in the area. North of the gravity high, a gravity low extends southwest parallel to valley trends, and includes a localized 150-μGal gravity low occurring in the northeast section.

The depths to bedrock derived from the wells in the area are highly variable and range from 24.9 to over 136.5 ft. Four wells located within the gravity high show bedrock depths ranging from 31.5 to 42 ft. Twenty-four wells located in the southwest trending gravity low show bedrock depths ranging from 24.9 to 136.5 ft with an average of 53 ft. On average, the bedrock is 18 ft deeper within the gravity low compared with the depths observed within the gravity high. The bedrock depths within the gravity low are extremely variable with depth differences up to 112 ft over a lateral distance of 120 ft.

The well logs indicate cherty-clay overlying the dolomite bedrock and the presence of water-filled and mud-filled cavities within the bedrock up to 17.8 ft thick. The variable bedrock depths and cavities are evidence for a highly karstified geology within the K-901 site. The southwest trending gravity low may represent a buried paleovalley with a high degree of karstification. More data are needed to investigate whether the southwest trending low is connected to the 700-μGal low observed in line 3.

# 5. CONCLUSIONS AND RECOMMENDATIONS

The gravity profile lines and contour map in the K-25 area show anomalies that are related to the local geology, regolith thickness, and karst. Gravitational gradients are observed at the mapped locations of the Whiteoak Mountain fault, the syncline axis, and the contact between the Knox Group and Chickamauga Supergroup, and are modeled as contrasting bedrock densities. Low gravity values north of the syncline axis may be related to Chickamauga bedrock that is more karstified than the Chickamauga bedrock south of the syncline axis. The gravity suggests that the thin, fault-bounded slice of the Rome Formation (Cr) mapped east of the syncline, may in fact be dissected by a northwest striking fault. It is possible that Conasauga Group shale lies northeast of the proposed fault and that the modeled karstified Chickamauga bedrock continues east beneath the Rome slice.

Localized gravity lows are modeled as regolith thickness variations and mud-filled cavities throughout the study area. A large gravity low within the syncline is interpreted as an area of thick regolith cover. Conversely, two major gravity lows located near the Kingsport Formation (Ok) and Mascot Dolomite (Oma) contact are interpreted as concentrations of mud-filled cavities. If connected, the cavities may collectively serve as a major east-to-west groundwater conduit. Additional gravity lines across the Kingsport Formation (Ok) and Mascot Dolomite (Oma) will help to define the continuity of the modeled karst conduit. The modeled cavities are located near mapped sinkholes, which may represent the surface expression of the karstified bedrock. A smaller gravity low observed along line 1 is modeled as a mud-filled cavity within Chickamauga bedrock that may be related to a recent road collapse at this location.

The gravity anomalies modeled in this study point to specific locations that should be investigated further, such as the large anomalies observed along lines 1 and 3, and other smaller anomalies modeled as mud-filled cavities. The nonuniqueness of gravity data modeling limits the interpretation of the anomalies, and additional geophysical methods and drilling should be employed to further constrain the gravity models.

# 6. REFERENCES

Bailey, Z. C., and Withington, D. B., 1988, Well construction, lithology, and geophysical logs for boreholes in Bear Creek Valley near Oak Ridge, TN: U.S. Geological Survey Water-Resources Invest. Rep. 88-4068, Nashville, 21 pp.

Butler, D. K., 1991, Tutorial -- Engineering and environmental applications of microgravimetry, Proceedings of the Symposium on the Application of Geophysics to Engineering and Environmental Problems, The Society of Engineering and Mineral Exploration Geophysicists, 139-246.

Carpenter, P. J., Doll, W. E., and Kaufmann, R. D., 1995, Geophysical surveys over karst features near the Oak Ridge Y-12 Plant, Oak Ridge, Tennessee, Y/ER-200, Oak Ridge Y-12 Pant, Oak Ridge, TN.

Coleman, P. R., Durfee, R. C., Poling, R. S., and Zondlo, T. F., in preparation, A study of historic change for the DOE K-25 Site from the preconstruction period to current landform conditions to assist in environmental restoration assessments, Oak Ridge, TN.

Coleman Energy & Environmental Systems - Blackhawk Geosciences Division, 1994, Microgravity survey of K-1070-A burial ground at the Oak Ridge K-25 Site, Oak Ridge, Tennessee, for Science Applications International Corporation, Oak Ridge, TN.

Geraghty & Miller, Inc., 1989, Hydrogeology of the Oak Ridge Gaseous Diffusion Plant, Final Report, K/SUB/85-22224/12, Prepared for Martin Marietta Energy Systems, Inc., Oak Ridge, TN.

Golden Software, Inc, 1994, Surfer for Windows, Golden, CO.

Hammer, S., 1939, Terrain corrections for gravimeter stations, Geophysics, **4**, 184-194.

Hatcher, Jr., R. D., Lemiszki, P. J., Dreier, R. B., Ketelle, R. H., Lee, R. R., Leitzke, D. A., McMaster, W. M., Foreman, J. L., and Lee, S. Y., 1992, Status report on the geology of the Oak Ridge Reservation, ORNL/TM-12074, Oak Ridge National Laboratory, Oak Ridge, TN.

Johnson Jr., R. W., and Stearns, R. G., 1967, Bouguer gravity anomaly map of Tennessee, State of Tennessee Department of Conservation, Division of Geology.

LaCoste & Romberg, 1991, Instruction manual, model G and D gravity meters, LaCoste and Romberg Gravity Meters, Inc.

Lemiszki, P. J., 1994, Geological mapping of the Oak Ridge K-25 Site, Oak Ridge, Tennessee, Martin Marietta Energy Systems, Inc., Environmental Restoration Program Report K/ER-111.

Lemiszki, P. J., Zerr, B. A., Herzog, M. C., and Zondlo, T. F., 1995, A karst inventory of the Oak Ridge area, Tennessee: The first step towards characterizing hazardous waste sites in carbonate terrains, Geological Society of America Abstracts with Programs, V. 27, p. 87.

Pannatier, Y., 1996, VARIOWIN: Software for spatial data analysis in 2D, Springer-Verlag, New York, NY.

Saltus, R. W., and Blakely, R. J., 1993, HYPERMAG, An interactive, 2- and 2 ½-dimensional gravity and magnetic modeling program: version 3.5, U.S. Geological Survey, Open-File report 93-287.

Shevenell, L. A., 1994, Chemical characteristics of waters in karst formations at the Oak Ridge Y-12 Plant, T/TS-1001, Martin Marietta Energy Systems, Inc., Oak Ridge Y-12 Plant, Oak Ridge, TN.

Taylor Jr., H. M., 1975, Foundation design for static loadings; special site investigation -conceptual design; gas centrifuge plant; first priority and Bear Creek sites; ORGDP area, Oak Ridge, Tennessee, U.S. Army Engineer Waterways Experiment Station, Soils and Pavements Laboratory.

Telford, W. M., Geldart, L. P., Sheriff, R. E., and Keys, D. A., 1976, Applied geophysics, Cambridge University Press.

Watkins, J. S., 1964, Regional geologic implications of the gravity and magnetic fields of a part of eastern Tennessee and southern Kentucky, Geological Survey Professional Paper 516-A, United States Government Printing Office, Washington, D.C.

Wilson, J. M., and Ketelle, R. H., 1992, K-1070-A gravity survey, MMHE 1.11-001, Environmental Consulting Engineers, Inc., for K-25 Site E.R. Program, Oak Ridge, TN.

# APPENDIX A. BASE STATIONS

This appendix lists the locations and simple Bouguer gravity (S.B.G.) values for the base stations used in the gravity survey. The Bouguer density used to calculate the simple Bouguer gravity is 2.4 g/cc. The easting and northing are reported in K-25 grid coordinates. A complete list of the simple Bouguer values, terrain corrections, and regional-corrected Bouguer values for all of the stations is available in the OREIS data base.

| STATION | EASTING | NORTHING | ELEV. | S.B.G. |
|---|---|---|---|---|
| UT | ------ | ------ | 948.16 | -57.348 |

*{All readings are tied to the U.T. base station. Located in cement outside front entrance of geology building. Marked as U.S. Coast and Geodetic Survey Benchmark #Z189. LON: 83.925333 ° W LAT: 35.956666 ° N Absolute gravity: 979697.14 mGals}*

ESD ------ ------ 806.68 -63.043
*{Reading obtained here for convenient reoccupation in the future. Located at the GPS benchmark near the west entrance of ORNL. LON: 84.3222458 ° W*
*LAT: 35.9252933 ° N Absolute gravity: 979697.721 mGals}*

Base0 21703 -30668 790 -63.493
*{This base station was reoccuppied at least twice a day. Located in the southeast corner of room 103, Bldg. 3504, ORNL. The location and elevation are estimates, so the S.B.G. is also an estimate at this station.}*

Base1 4770.11 -18202.71 820.63 -58.933
*{line 1, station 101}*

Base1a 4363.67 -17668.66 771.83 -59.283
*{line 1, station 600}*

Base2 3474.09 -27591.94 801.80 -63.425
*{line 2, station 56}*

Base3a -1530 -28036 764.40 -61.717
*{on median near station 339; estimated location and elevation}*

Base3b -2753 -27854 754.17 -61.601
*{on concrete slab near station 207; estimated location and elevation}*

Base3c -3973 -26880 753.45 -61.212
*{on railroad tie near station 208; estimated location and elevation}*

Base3d -4972.36 -25139.55 767.55 -59.755
*{line 3, station 434}*

Base3e -5022.69 -23060.70 767.05 -58.801
*{line3, station 476}*

Base9 -5555 -22291 799.20 -58.246
*{on northeast corner of the slab for well UNW31, estimated location and elevation}*

Base10 1685 -28511 769.00 -62.999
*{on concrete slab near station 1017, estimated location and elevation}*

BaseC1 -444.00 -26388.00 778.70 -61.960
*{catch basin station 13152}*

# DISTRIBUTION

1. S. B. Ahmed
2. L. V. Asplund
3–4. W. E. Doll
5. R. B. Dreier
6–10. R. D. Kaufmann
11. P. J. Lemiszki
12. D. M. Matteo
13. C. A. Motley
14. J. E. Nyquist
15–16. P. T. Owen
17. J. V. Spence
18. A. S. Quist
19. R. S. Poling
20. T. F. Zondlo
21. Central Research Library
22. ER Central Doc. Mgmt. Center—RC
23. B. S. Murray, SAIC, P.O. Box 2502, Oak Ridge Turnpike, Oak Ridge, TN 37832
24. J. Wilson, Environmental Consulting Engineers, P.O. Box 22668, Knoxville, TN 37933